Journal of Industrial and Engineering Chemistry

Tunable HMF hydrogenation to furan diols in a flow reactor using Ru/C as catalyst

--Manuscript Draft--

Manuscript Number:	
Article Type:	Full Length Article
Section/Category:	Catalyst
Keywords:	5-hydroxymethylfurfural; Tunable hydrogenation; Aqueous-phase; 2,5-bis(hydroxymethyl)furan; 2,5-bis(hydroxymethyl)tetrahydrofuran; Flow reactor
Corresponding Author:	Claudia Antonetti University of Pisa Pisa, ITALY
First Author:	Claudia Antonetti
Order of Authors:	Claudia Antonetti
	Sara Fulignati
	Erwin Wilbers
	Domenico Licursi
	Hero Jan Heeres
	Anna Maria Raspolli Galletti
Abstract:	5-hydroxymethylfurfural (HMF), accessible from various feedstocks, represents an important renewable platform-chemical, precursor for valuable biofuels and bio-based chemicals. In this work, the continuous hydrogenation of an aqueous solution of HMF to give strategic monomers, 2,5-bis(hydroxymethyl)furan (BHMF) and 2,5-bis(hydroxymethyl)tetrahydrofuran (BHMTHF) was investigated in a continuous flow reactor adopting a commercial Ru/C (5 wt%) as catalyst. The influence of the main process variables on products yield and selectivity was studied and optimized. The highest BHMF and BHMTHF yields of 87.9 and 93.7 mol%, respectively, were achieved by tuning the catalyst contact time, keeping all other variables constant (temperature, pressure, hydrogen flow rate, initial HMF concentration). Intraparticle diffusion limitation for hydrogen and HMF was shown to occur at some of the tested conditions by performing the HMF hydrogenation with different catalyst particle sizes, confirmed by calculations. Constant catalyst activity was observed up to 6 h time-on-stream and then gradually reduced. Fresh and spent catalyst characterization showed no significant sintering and negligible leaching of ruthenium during time-on-stream. A decrease of the specific surface area was observed, mainly due to humin deposition which is likely the reason for catalyst deactivation. Catalyst performance could be restored to initial values by a thorough washing of the catalyst.
Suggested Reviewers:	Jean-Stepḥane Condoret jeanstephane.condoret@ensiacet.fr He is an expert in this field
	Martino Di Serio diserio@unina.it He is an expert in this field
	Xing Tang x.tang@xmu.edu.cn He is an expert in this field
	Pierluigi Barbaro pbarbaro@iccom.cnr.it He is an expert in this field.

UNIVERSITÀ DI PISA

DIPARTIMENTO DI CHIMICA E CHIMICA INDUSTRIALE

Via G. Moruzzi, 13 - 56124 Pisa (Italy)

Centralino - Tel. (050) - 2219001

Prof. Claudia Antonetti
Tel. (050) – 22 19373
FAX (050) – 2220673
e-mail: claudia.antonetti@unipi.it

Pisa, 11/2/2021

Dear Editor,

enclosed you find our paper **"Tunable HMF hydrogenation to furan diols in a flow reactor using Ru/C as catalyst"** for publication in "Journal of Industrial and Engineering Chemistry".

This submission is original and it is not under consideration for publication elsewhere. The authors are aware of the submission and agree to its publication.

The paper studies the selective hydrogenation of 5-hydroxymethylfurfural (HMF) to either 2,5-bis(hydroxymethyl)furan (BHMF) or 2,5-bis(hydroxymethyl)tetrahydrofuran (BHMTHF) in a continuous flow reactor using the commercial 5 wt% Ru/C catalyst in water. The influence of relevant reaction parameters for the selective synthesis of each diol was determined and optimized. The highest BHMF and BHMTHF yields of 88.0 and 93.7 mol%, respectively, were obtained by simply tuning the catalyst contact time, keeping all other reaction parameters at the same values. This approach is very promising from an application perspective, because the catalyst contact time can be easily modified by changing the adopted feed flow, thus allowing the selective synthesis of each diol without changing the type of catalyst and reaction conditions. This represents a novel aspect in this research field. Fresh and spent catalyst characterization showed no significant sintering and negligible leaching of ruthenium during time-on-stream, mainly claiming the humin deposition as the reason for catalyst deactivation. However, catalyst performance could be restored to initial values by a washing procedure.

Yours faithfully,

Prof. Claudia Antonetti

Declaration of interests

☒The authors declare that they have no known competing financial interests or personal relationships that could have appeared to influence the work reported in this paper.

☐The authors declare the following financial interests/personal relationships which may be considered as potential competing interests:

Graphical Abstract

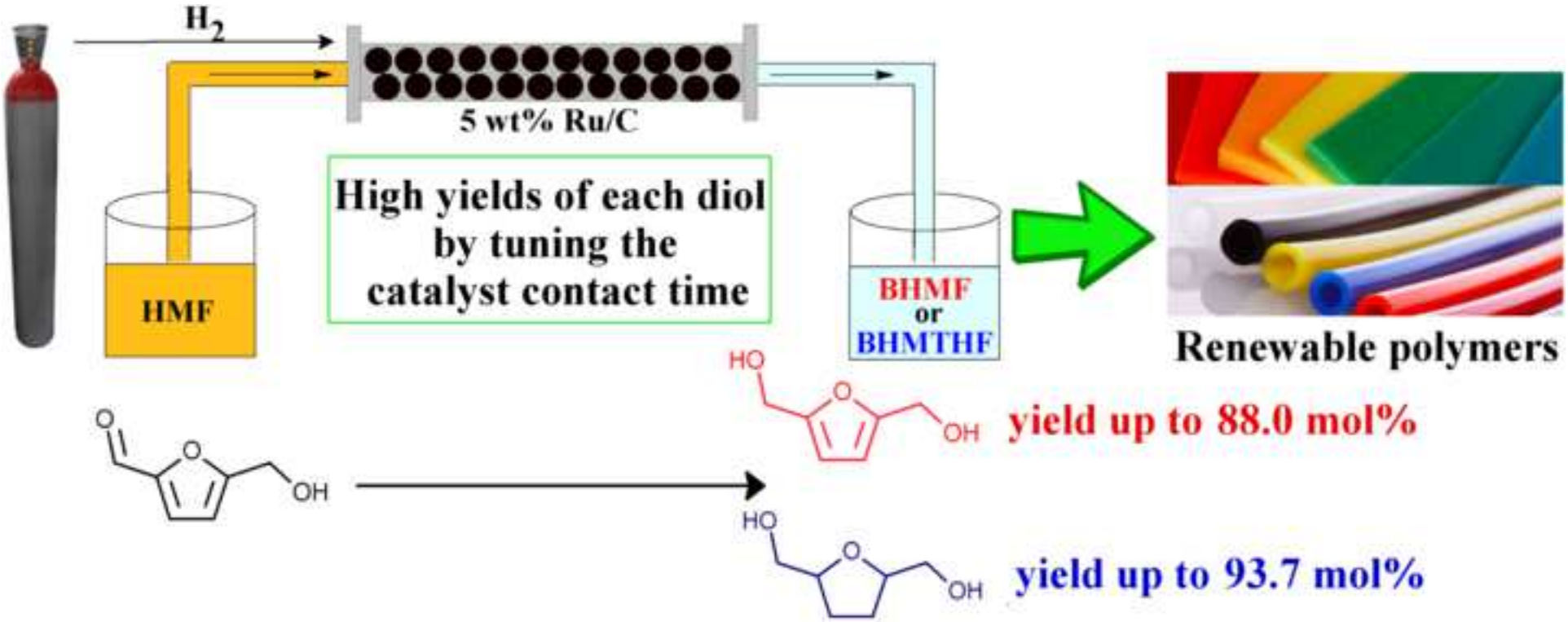

Highlights

- The hydrogenation of HMF to furan diols was studied and optimized in flow reactor.
- The commercial Ru/C was an efficient catalyst for the BHMF and BHMTHF synthesis.
- The highest BHMF and BHMTHF yields were ascertained only tuning the contact time.
- The catalyst was stable up to 6 h and easily reactivable through acetone washing.
- Internal mass transfer limitations occurred and affected the overall reaction rate.

Tunable HMF hydrogenation to furan diols in a flow reactor using Ru/C as catalyst

Sara Fulignati[a], Claudia Antonetti[a]*, Erwin Wilbers[b], Domenico Licursi[a], Hero Jan Heeres[b], Anna Maria Raspolli Galletti[a]

[a] *Department of Chemistry and Industrial Chemistry, University of Pisa, Via G. Moruzzi 13, 56124, Pisa, Italy.*

[b] *Green Chemical Reaction Engineering, ENTEG, University of Groningen, Nijenborgh 4, 9747 AG Groningen, The Netherlands.*

*Corresponding author, e-mail: claudia.antonetti@unipi.it

Abstract

5-hydroxymethylfurfural (HMF), accessible from various feedstocks, represents an important renewable platform-chemical, precursor for valuable biofuels and bio-based chemicals. In this work, the continuous hydrogenation of an aqueous solution of HMF to give strategic monomers, 2,5-bis(hydroxymethyl)furan (BHMF) and 2,5-bis(hydroxymethyl)tetrahydrofuran (BHMTHF) was investigated in a continuous flow reactor adopting a commercial Ru/C (5 wt%) as catalyst. The influence of the main process variables on products yield and selectivity was studied and optimized. The highest BHMF and BHMTHF yields of 87.9 and 93.7 mol%, respectively, were achieved by tuning the catalyst contact time, keeping all other variables constant (temperature, pressure, hydrogen flow rate, initial HMF concentration). Intraparticle diffusion limitation for hydrogen and HMF was shown to occur at some of the tested conditions by performing the HMF hydrogenation with different catalyst particle sizes, confirmed by calculations. Constant catalyst activity was observed up to 6 h time-on-stream and then gradually reduced. Fresh and spent catalyst characterization showed no significant sintering and negligible leaching of ruthenium during

time-on-stream. A decrease of the specific surface area was observed, mainly due to humin deposition which is likely the reason for catalyst deactivation. Catalyst performance could be restored to initial values by a thorough washing of the catalyst.

Keywords

5-hydroxymethylfurfural; Tunable hydrogenation; Aqueous-phase; 2,5-bis(hydroxymethyl)furan; 2,5-bis(hydroxymethyl)tetrahydrofuran; Flow reactor.

1. Introduction

The depletion of fossil resources together with their contribution to environmental issues related to CO_2 emissions have stimulated research towards the synthesis of chemicals from renewable resources, such as lignocellulosic biomasses [1]. In this regard, 5-hydroxymethylfurfural (HMF) is a key platform-chemical, accessible from monosaccharides and polysaccharides [2–8], and the precursor for several value-added products, such as 2,5-furandicarboxylic acid (FDCA), 2,5-dimethylfuran (DMF), 2,5-bis(hydroxymethyl)furan (BHMF), and 2,5-bis(hydroxymethyl)tetrahydrofuran (BHMTHF) [9–15]. The two last compounds are obtained from the hydrogenation of the aldehyde group (BHMF) and also of the furanic ring (BHMTHF), as reported in Scheme 1.

Scheme 1, near here

Both are considered highly important intermediates due to their promising applications as valuable monomers [16] as well as precursors for other important monomers that, up to now, are obtained from fossil resources, such as caprolactam and 1,6-hexanediol [17–19]. Generally, HMF hydrogenations to BHMF and BHMTHF are carried out using heterogeneous catalysts, in particular noble metals supported on oxides, polymers, or carbon species, mainly tested in batch reactors [14,20–22]. However, this reactor set-up is not suitable for industrial

applications where continuous operations are preferred [23–26]. Only recently, experimental studies using continuous set-ups have been reported for the synthesis of biobased chemicals [27], such as for the hydrogenation of levulinic acid [28–30], furfural [31–33] and HMF [19,34–42]. Regarding HMF hydrogenation in flow, the most investigated reaction involves the synthesis of DMF [34–38] and only limited researches deal with the synthesis of BHMF and BHMTHF [19,39–42]. An overview of the HMF hydrogenation carried out in flow reactors is given in Table 1.

Table 1, near here

Regarding the HMF hydrogenation to furan diols, Kumalaputri *et al.* carried out the hydrogenation of HMF to BHMF in ethanol employing Cu doped porous metal oxides (PMO) with an amount of Cu of 7.6 wt% (7.6 wt% Cu-PMO) as the catalyst [39]. At the optimized reaction conditions, the BHMF yield of 80 mol% was reported together with the HMF conversion of 90 mol%. Hu *et al.* performed the same reaction in ethanol using a more concentrated HMF solution and 5 wt% Cu/Al_2O_3 doped with 1.5 wt% of potassium (to increase dispersion and reduce support acidity) as the catalyst [40]. Under the optimized conditions, the authors reported the BHMF yield of about 99 mol% at full HMF conversion. The hydrogenation of HMF to BHMF and BHMTHF in flow was investigated also in water, which is considered the most sustainable solvent in terms of toxicity and price. Lima *et al.* tested several commercial catalysts for the hydrogenation of HMF in an aqueous solution to BHMF and BHMTHF [41]. The authors found that RANEY Cu was the best catalyst for the synthesis of BHMF, affording the highest yield of 86 mol%, although interesting yields of BHMTHF (about 76 mol%) could be obtained only adopting a two-step procedure in which RANEY Cu was used in the first step for the hydrogenation of HMF to BHMF and RANEY Ni for the second step from BHMF to BHMTHF. In fact, the authors synthesized BHMTHF from the crude BHMF solution under the same reaction conditions of the first step, achieving

the BHMTHF yield of 76 mol% respect to the starting HMF. Xiao *et al.* performed the synthesis of BHMTHF reaching quantitative yields from an aqueous HMF solution using 0.6 wt% Pd/SiO_2 as the catalyst [19].

We here report studies on BHMF and BHMTHF synthesis using aqueous HMF solutions as feed in a flow reactor. In particular, and this is an absolute novelty of this paper, this research is focused on the possibility to achieve high yields of each diol without major modifications regarding process conditions. For this purpose, a commercial catalyst (5 wt% Ru/C), already successfully used by our research group in batch reactor, was employed [14,43,44]. As consequence, the process could become versatile and interesting under an industrial perspective because in this way it is made adaptable to the market request, reducing equipment, investment and production costs.

2. Experimental

2.1 Materials

HMF (99%) was supplied by Sigma-Aldrich. BHMF (98%) was purchased from Toronto Research Chemicals. BHMTHF (95%) was provided by GLSyntech. Ru/C (5 wt%), silicon carbide, and dichloromethane (99.9%) were purchased from Sigma-Aldrich. Milli-Q water was employed to prepare the solutions.

2.2 HMF hydrogenation in the flow reactor

The set-up of the flow reactor employed for HMF hydrogenation was composed of a feeding section, a preheater, a reactor (ID = 0.7 cm; L = 14.2 cm), a gas-liquid separator, and an auto-sampler (Scheme S1). In a standard run, the HMF aqueous solution was prepared and it was transferred in the feed vessel. The proper amount of catalyst (5 wt% Ru/C) was mixed with silicon carbide (inert filler), and loaded into the reactor. Subsequently, the reactor was closed and the HMF solution was fed through a piston pump with a volumetric feed flow rate of 1

ml/min. Catalyst contact times were varied by modifying the catalyst intake while keeping the volumetric feed flow rate constant. The pressure, monitored at two positions (before the preheater and immediately after the reactor), was set to the desired value through a back pressure valve. The reactor and preheater were heated electrically to the pre-determined temperature, which was measured at the entrance and exit of the reactor through two thermocouples. Subsequently, the hydrogen flow, fed directly from the cylinder, was started and monitored by a flow controller. When the temperature reached the preset value, the reaction time was set to zero (t = 0 h). At different runtimes, liquid samples were collected by an in-house made auto-sampler and analysed by HPLC. The considered process variables and their ranges are reported in Table 2.

Table 2, near here

For the recycling tests, the employed catalyst was recovered from the reactor, washed under stirring with acetone at room temperature, filtered, dried, and used in a subsequent run.

2.3 Product analysis by HPLC

The liquid samples were filtered through a syringe filter (0.45 μm) and analyzed using an HPLC Agilent Technologies 1260 Infinity equipped with a Bio-Rad Aminex HPX-87H (300 × 7.8 mm) column kept at 60 °C, and employing 0.005 M H_2SO_4 as the mobile phase (flow rate: 0.55 ml/min). The concentrations of the products were determined from calibration curves obtained with standard solutions of different concentrations.

2.4 Product analysis by GC-MS

The products formed during the hydrogenation of HMF in flow were identified by gas chromatography coupled with a mass spectrometer (GC-MS). Before the analysis, the aqueous solution was extracted three times with dichloromethane, the organic phase was concentrated under vacuum and injected. A GC-MS (Hewlett Packard 5973-6890) equipped

with a Restek RTX-1701 capillary column (30 m × 0.25 mm i.d. and 0.25 μm film 14%-cyanopropylphenyl/86%-dimethylpolysiloxane) was employed for the analysis. The temperatures of the injector and detector were set at 250 °C and 285 °C, respectively. The following temperature program was used: 40 °C isothermal for 10 min and then heating up with a heating rate of 10 °C/min up to 250 °C.

2.5 Catalyst characterization

Transmission Electron Microscopy (TEM) measurements in bright field mode were carried out with a CM12 microscope (Philips), operating at 120 keV. The catalysts were suspended in ethanol by ultra-sonication and the obtained sample was dropped onto carbon coated 400 mesh copper grids. Images were taken on a slow scanning CCD camera. The ruthenium particle size distribution was evaluated by measuring the particle diameter of a large number of individual particles using Nano Measurer 1.2 software.

Nitrogen physisorption analyses were performed using a Micromeritics ASAP 2020 at −196.2 °C. Before measurement, the samples were degassed under vacuum at 150 °C for 6 h. The surface area was estimated using the standard BET method.

The ruthenium content in the liquid sample after the reaction was determined by inductively coupled plasma-optical emission spectrometry (ICP-OES) using an Optima 7000 DV (PerkinElmer) analyzer equipped with a CCD array detector.

2.6 Definitions

The HMF conversion (X_{HMF}, mol%), and the yields of BHMF (Y_{BHMF}, mol%) and BHMTHF (Y_{BHMTHF}, mol%) were calculated according to equations 1-3:

$$X_{HMF} = \frac{C_{HMF}^{in} - C_{HMF}^{out}}{C_{HMF}^{in}} \cdot 100\% \qquad \text{(eq.1)}$$

$$Y_{BHMF} = \frac{C_{BHMF}^{out}}{C_{HMF}^{in}} \cdot 100\% \quad \text{(eq.2)}$$

$$Y_{BHMTHF} = \frac{C_{BHMTHF}^{out}}{C_{HMF}^{in}} \cdot 100\% \quad \text{(eq.3)}$$

where C_{HMF}^{in} is the inlet concentration of HMF (mol/l); C_{HMF}^{out}, C_{BHMF}^{out} and C_{BHMTHF}^{out} are the concentration of HMF, BHMF, and BHMTHF in the outlet flow (mol/l), respectively.

The carbon balance (mol%) was evaluated by comparing the sum of the molar concentration of unconverted HMF, the molar concentrations of products (BHMF and BHMTHF), and the molar concentrations of quantified by-products in the outlet flow with the starting concentration of HMF, according to equation 4:

$$Carbon\ balance = \frac{C_{HMF}^{out} + C_{BHMF}^{out} + C_{BHMTHF}^{out} + C_{others}^{out}}{C_{HMF}^{in}} \cdot 100\% \quad \text{(eq.4)}$$

where C_{others}^{out} is the concentration of quantified by-products, in particular tetrahydrofurfuryl alcohol and 1,2-pentandiol, in the outlet flow (mol/l).

The catalyst contact time (CCT, $g_{cat} \times min/g_{HMF}$) was calculated according to equation 5:

$$CCT = \frac{m_{catalyst}}{f \cdot c_{HMF}} \quad \text{(eq.5)}$$

where $m_{catalyst}$ is the amount (g) of the employed catalyst, f is the volumetric flow rate of the feed (ml/min), and c_{HMF} is the concentration of HMF (g/ml) in the feed.

3. Results and discussion

3.1 Preliminary experiments of HMF hydrogenation in the flow reactor

Preliminary experiments (100 °C, 50 bar, CCT of 10 $g_{cat} \times min/g_{HMF}$, H_2 flow of 100 ml/min, liquid flow of 1 ml/min and HMF concentration of 0.1 wt% corresponding to 7.9 mM) were performed in triplicate in order to obtain information on the stability of the catalyst (5 wt%

Ru/C) and the reproducibility of the experiments. The results for a 50 (A) and 6 h (B) time-on-stream experiment with the error bars are reported in Figure 1.

Figure 1, near here

Reproducibility was good and standard deviations in the HMF, BHMF, and BHMTHF concentrations were low (relative error of 7%). However, the concentration versus time curves indicate that catalyst stability was limited. In fact, high activity was found at the beginning of the reaction, followed by a small decay after 2 h. Subsequently, activity was almost constant between 2 and 6 h, followed by a decrease when prolonging the time-on-stream (Figure 1A). For further experiments, the HMF conversion and product yields between 2 and 6 h were selected as being representative of the steady-state performance of the reactor (Figure 1B). As such, the average HMF conversion and average yields of the products were calculated for the liquid samples collected between 2 and 6 h of time-on-stream at time lapses of 1 h. Under the reaction conditions employed in these preliminary experiments, the HMF conversion of 62.8 mol% was obtained with BHMF as the major product (58.5 mol% yield). BHMTHF was only obtained in low yield (1.8 mol%) together with trace amounts of other by-products (HPLC). After this preliminary study, the influence of the relevant reaction conditions on the selective synthesis of each diol was investigated in more detail.

3.2 Optimization of reaction parameters for the selective hydrogenation of HMF to a specific diol

The role of the CCT on catalyst performance was studied by performing the HMF hydrogenation with different catalyst intakes, keeping the liquid flow rate constant (1 ml/min) and working at the same reaction conditions (100 °C, 50 bar, H_2 flow of 100 ml/min and the HMF feed concentration of 0.1 wt%). The results are provided in Figure 2.

Figure 2, near here

Complete HMF conversion was only possible when the CCT was larger than 50 g_{cat}×min/g_{HMF}. Moreover, at CCT values lower than 50 g_{cat}×min/g_{HMF} the main product was BHMF thus the selective hydrogenation of the aldehyde group was only possible at short contact times between the substrate and the catalyst. The highest BHMF yield of 88.0 mol% was obtained at 20 g_{cat}×min/g_{HMF}. At higher CCT values, hydrogenation of the furan ring occurred and the BHMTHF yield increased from 6.2 mol% at 20 g_{cat}×min/g_{HMF} to 93.7 mol% at 300 g_{cat}×min/g_{HMF}, which represents the highest value obtained in this study. The carbon balance ranged between 98.1 and 93.2 mol% and slightly decreased at higher CCT values. Thus, it can be concluded that the optimum CCT is 20 g_{cat}×min/g_{HMF} for the synthesis of BHMF and 300 g_{cat}×min/g_{HMF} for BHMTHF.

The effect of temperature (60–120 °C) on product selectivity and yield was studied at the above CCT values and the results are reported in Figure 3.

Figure 3, near here

Working at CCT of 20 g_{cat}×min/g_{HMF} (Figure 3A), the HMF conversion versus temperature showed an optimum at 100 °C, reaching 96.0 mol%, whereas it decreased at 120 °C. Humins formation and their subsequent deposition on the catalyst surface, expected to be favoured at higher temperatures, may lead to pore blockage of the catalysts and therefore to a reduction in the overall rate. An increase of the extend of the humin formation rate at 120 °C was also confirmed by a reduction in the carbon balance closure (humins are not included, only water-soluble low molecular weight compounds, see eq. 4). A similar trend was found for the BHMF yield, which reached a maximum at 100 °C (88.0 mol%) and decreased at 120 °C. Moreover, when performing the reaction at 120 °C, traces of tetrahydrofurfuryl alcohol and 1,2-pentandiol were detected. These by-products derived from HMF decarbonylation to the intermediate furfuryl alcohol, which is known to be promoted at higher temperatures (Scheme S2) [36,45]. The successive hydrogenation of the furanic ring of furfuryl alcohol gives

tetrahydrofurfuryl alcohol, which then undergoes the ring-opening reaction to 1,2-pentandiol [46]. Götz *et al.* showed that furfuryl alcohol can also directly be converted to 1,2-pentandiol through a hydrogenolysis mechanism, for instance when using ruthenium catalysts in water [47]. Moreover, tetrahydrofurfuryl alcohol can be obtained from the C-C bond cleavage of BHMTHF (Scheme S2) [14,48].

When using a CCT value of 300 g_{cat}×min/g_{HMF} (Figure 3B), quantitative HMF conversion was obtained at all temperatures in the range 60–120 °C. The BHMTHF yield showed a maximum value (93.7 mol%) at 100 °C. However, at 120 °C the BHMTHF yield markedly dropped, again likely due to humin formation. Also in this case, tetrahydrofurfuryl alcohol and 1,2-pentandiol were formed in yields of 14.8 and 11.2 mol%, respectively. Regarding the carbon balance, as expected it decreased when increasing the temperature from 100 to 120 °C, due to the formation of humins. However, both in Figures 3A and B the carbon balance increased from 60 to 100 °C. A possible explanation is HMF adsorption on the catalyst surface [49], which leads to an overestimation of the HMF conversion. This hypothesis was proven by performing separate adsorption experiments of HMF (1 g/L) with Ru/C and SiC (room temperature, 20 min). Analysis of the mixtures showed that the HMF concentration was lower than the initial value for Ru/C (0.4 g/L), whereas the concentration was unchanged in the presence of SiC, thus confirming the high affinity of Ru/C for HMF.

The effect of the hydrogen pressure on HMF conversion and products yield when using CCT values of 20 g_{cat}×min/g_{HMF} (A) and 300 g_{cat}×min/g_{HMF} (B) at 100 °C are given in Figure 4.

Figure 4, near here

Only at the lowest CCT value an effect of hydrogen pressure on HMF conversion was observed and both the BHMF yield and HMF conversion increased at higher pressures (10 to 50 bar, Figure 4A). At the higher CCT value (Figure 4B), the HMF conversion was complete already at 10 bar. At higher pressures, hydrogenation of the furan ring of BHMF was

promoted giving BHMTHF as the major product (93.7 mol% at 50 bar). Moreover, Figure 4 shows that the carbon balance closure was only slightly reduced at higher pressures, indicating that by-product formation is not markedly influenced by this parameter.

Analogous trends were also found when investigating the influence of the hydrogen flow rate (Figure S1). In this case, a flow of 100 ml/min gave the best results for each diol. For all experiments, hydrogen was present in molar excess with respect to HMF, and as such an effect of hydrogen flow rate on catalyst performance is not expected. Thus, it more likely that this is due to mass transfer issues when working at low hydrogen flow rates due to negative effects on the volumetric mass transfer coefficients [50].

In conclusion, the selective hydrogenation of HMF to either BHMF or BHMTHF in a flow reactor with the same commercial catalyst Ru/C was demonstrated for the first time and their yields were optimized [19,39–41]. Moreover, the selectivity to either BHMF or BHMTHF resulted tunable with the CCT, keeping all other reaction conditions constant (temperature, pressure, and hydrogen flow rate).

3.3 Effect of HMF feed concentration

From an economic perspective, it is advantageous to work at the highest possible HMF feed concentrations, as this will reduce purification and solvent recycle costs and increase the process productivity (kg product/m^3×h). Therefore, the syntheses of BHMF and BHMTHF were carried out under the respective best reaction conditions identified in the previous paragraph employing higher feed concentrations of HMF (max 2.0 wt%).

Figure 5, near here

In both cases, higher HMF feed concentrations had a negative effect on conversion and product selectivity. For BHMF synthesis (Figure 5A), an increase in HMF feed concentration led to a marked drop in HMF conversion and BHMF yield, from 88.0 mol% at the HMF feed

concentration of 0.1 wt% to 17.5 mol% at 2.0 wt%. This is likely due to a combination of a short contact time between the substrate and the active sites and a higher formation rate of humins promoted at higher HMF concentrations [51], confirmed by a reduction in the carbon balance closure. A similar trend was found when using process conditions optimal for BHMTHF synthesis (Figure 5B). Besides, by-products, such as 1,2-pentandiol and tetrahydrofurfuryl alcohol, were detected in yields of about 4.0 and 3.0 mol%, respectively. Moreover, other not quantified soluble by-products were detected and identified by GC-MS analysis. Examples are furfuryl alcohol, 1,5-pentanediol, 1,2,6-hexanetriol, tetrahydropyran-2-methanol, 1,2-hexanediol, and 1,5-hexanediol. These can originate from the decomposition/hydrogenation of HMF and BHMTHF (Scheme S3). For instance as previously reported, tetrahydrofurfuryl alcohol can be formed by C-C bond cleavage of BHMTHF [48] and the hydrogenation of furfuryl alcohol, originating from HMF decarbonylation [45]. Both furfuryl alcohol and tetrahydrofurfuryl alcohol can undergo the ring-opening reaction leading to 1,2-pentandiol and/or 1,5-pentandiol [46,52,53]. On the other hand, also BHMTHF is prone to ring-opening reactions leading, in this case, to 1,2,6-hexanetriol [46,54,55], which can be converted to tetrahydropyran-2-methanol [17,54,55] or 1,2-hexanediol and 1,5-hexanediol, through hydrogenolysis of the C-O bond [17,46,54]. Thus, when using a more concentrated HMF feed, condensation reactions to give humins as well as by-product formation reduce the chemoselectivity to the desired diols.

3.4 Internal mass transfer effects

HMF hydrogenation using a solid catalyst involves three phases system and thus the observed rate is determined by the intrinsic reaction rate and the rate of mass transfer of hydrogen and/or HMF to the active sites of the catalyst. In particular, both external mass transfer, responsible for the transport of soluble reagents in the liquid phase to the surface of the catalyst, and internal mass transfer, responsible for intraparticle transport, may limit the rate

of the overall reaction. Here, we have considered only the effect of intraparticle mass transfer on the overall reaction rate, as it is typically the most limiting for heterogeneous reaction systems [56]. Possible intraparticle mass transfer limitations of hydrogen and HMF were estimated using the Weisz-Prater criterium (eq. 6) [57].

$$N_{W-P} = \frac{-R_{\exp} \acute{} r_p^2}{C_s \acute{} D_{eff}} \qquad \text{(eq. 6)}$$

Here, R_{exp} is the experimentally observed reaction rate (mol/m^3_{cat} × s); r_p is the radius of catalyst particle (m); C_s is the concentration of the component at the catalyst surface (mol/m^3), D_{eff} is the effective diffusion coefficient of the component (m^2/s) and their expressions are reported in the Supplementary Data. In case the Weisz-Prater number is below 0.3, intraparticle mass transfer limitation of reagents is negligible. We have evaluated the Weisz-Prater number for all experiments and the details are provided in the Supplementary Data (Tables S1 and S2). Intraparticle mass transfer limitations were shown to be relevant for HMF and, in a few runs, also for hydrogen. Experimental confirmation for intraparticle mass transfer limitations was obtained by performing the reaction with Ru/C samples having different average particle sizes. For this purpose, the catalyst was sieved into two fractions, one having particles in the range of 25-75 μm and the second one with particles in the range of 150-200 μm. The two fractions were employed at the same reaction conditions used for the experiment reported in Figure 1 and the results are shown in Figure 6.

Figure 6, near here

The use of the smaller catalyst particles gave an improvement of HMF conversion of about 46.8 mol% respect to the larger ones, confirming that intraparticle mass transfer limitations affect the overall rates and thus the conversion/yield versus time-on-stream profiles. Such intraparticle mass transfer limitations have also been reported in the literature for several hydrogenations of biobased platform chemicals using Ru-based catalysts. Moreno-Marrodan

et al. obtained a 10 mol% higher LA conversion when the average particle size of a Ru/DOWEX 50WX2 catalyst was decreased from 276 to 84 μm [58], whereas Piskun *et al.* reported an improvement of 34 mol% for the LA conversion when a millimeter-sized Ru/C catalyst (1.25-2.50 mm) was crushed and sieved in a fraction having particle sizes between 0.5 and 0.6 mm [29].

3.5 Catalyst stability and recyclability

The catalytic activity was shown to decrease during extended time-on-stream (Figure 1, 50 h). The spent catalyst recovered from this experiment was characterized in details to get a better understanding of the deactivation mechanism. The surface area of the spent catalyst (136 m^2/g) was significantly lower than that of the fresh one (770 m^2/g). As ascertained in previous work [14], this is likely due to the deposition of humins and other compounds, such as HMF, on the catalyst surface that results in pore blockage. TEM analysis was carried out on the spent catalyst to verify the occurrence of ruthenium particle sintering. TEM micrographs and the ruthenium particles distributions for the fresh Ru/C and the spent Ru/C catalysts are provided in Figure S2. The fresh Ru/C catalyst was characterized by an average ruthenium particle size of 1.5 nm, in agreement with the results reported in the literature [59]. In the spent catalyst, some sintering was detected and the average ruthenium particle size increased up to 2.5 nm, in line with the Ru nanoparticle size of the spent catalyst recovered from batch hydrogenation of HMF [14]. It has been shown that water can facilitate Ru particle agglomeration and that this process already occurs at room temperature [60,61]. Leaching of ruthenium from the catalyst was also investigated through ICP analysis by determination of the Ru content in the liquid samples obtained during run reported in Figure 1. In all samples, the amount of ruthenium was below the detection limit, indicating that leaching of Ru was negligible.

These results indicate that deactivation of the catalyst during the time-on-stream is most likely related to the humin deposition on the surface. To verify whether this process is reversible, the spent catalyst was removed from the reactor, washed under stirring with acetone, filtered, dried under vacuum at 40 °C, and re-used in a subsequent run under the same reaction conditions of the experiment reported in Figure 1 (100 °C, 50 bar, 0.1 wt% of HMF, H_2 flow of 100 ml/min and liquid flow of 1 ml/min). The same procedure was adopted for a second recycle. The results of these recycling experiments are given in Figure 7.

Figure 7, near here

It is evident that an acetone wash led to a performance close to that found for the fresh catalyst. This confirms that deposition of humins and other compounds is most likely the major deactivation mechanism, whilst the slight increase in the ruthenium particle sizes does not affect the catalytic activity, as already indicated by previous works [14,43,44]. Besides, TEM analyses of the catalysts at the end of the first and second recycle did not show an appreciable increase in the average Ru nanoparticle size. In this regard, the washing reactivation procedure can be extended also to the catalysts recovered from the reactions optimised for the synthesis of BHMF and BHMTHF, which were carried out under the same reaction conditions but at different CCT, a parameter that does not significantly influence the humins formation as evidenced by the almost analogous trend of carbon balance (Figure 2).

4. Conclusions

We here report the selective hydrogenation of HMF to either 2,5-bis(hydroxymethyl)furan (BHMF) or 2,5-bis(hydroxymethyl)tetrahydrofuran (BHMTHF) in a continuous flow reactor using a commercial 5 wt% Ru/C catalyst in water. The influence of relevant reaction parameters for the selective synthesis of one of the diols was determined and optimized. The highest BHMF and BHMTHF yields of 88.0 and 93.7 mol%, respectively, were obtained by

tuning the catalyst contact time (CCT), keeping all other reaction parameters at the same values. This approach is very promising from an application perspective, because the CCT can be easily modified by changing the adopted feed flow, thus allowing for the selective synthesis of each diol without changing the type of catalyst and reaction conditions. TEM, ICP and nitrogen physisorption analyses proved that the experimentally observed deactivation of the catalyst after extended runtimes (> 6 h) was mainly due to the deposition of humins on the catalyst surface. However, recycle experiments showed that the catalyst can be efficiently reactivated by an acetone wash.

Acknowledgments

The project PRA_2018_26 of University of Pisa is gratefully acknowledged.

Appendix A. Supplementary data

Supplementary data related to this article can be found online at...

References

[1] R.A. Sheldon, ACS Sustainable Chem. Eng. 6 (2018) 4464–4480. http://doi.org/10.1021/acssuschemeng.8b00376

[2] C. Antonetti, M. Melloni, D. Licursi, S. Fulignati, E. Ribechini, S. Rivas, J.C. Parajó, F. Cavani, A.M. Raspolli Galletti, Appl. Catal. B: Env. 206 (2017) 364–377. http://doi.org/10.1016/j.apcatb.2017.01.056

[3] C. Antonetti, A.M. Raspolli Galletti, S. Fulignati, D. Licursi, Catal. Commun. 97 (2017) 146–150. http://doi.org/10.1016/j.catcom.2017.04.032

[4] H. Abou-Yousef, E.B. Hassan, J. Ind. Eng. Chem. 20 (2014) 1952–1957. http://doi.org/10.1016/j.jiec.2013.09.016

[5] G. Portillo Perez, A. Mukherjee, M.-J. Dumont, J. Ind. Eng. Chem. 70 (2019) 1–34. https://doi.org/10.1016/j.jiec.2018.10.002

[6] C. Antonetti, S. Fulignati, D. Licursi, A.M. Raspolli Galletti, ACS Sustainable Chem. Eng. 7 (2019) 6830–6838. http://doi.org/10.1021/acssuschemeng.8b06162

[7] C. Sonsiam, A. Kaewchada, S. Pumrod, A. Jaree, Chem. Eng. Process. 138 (2019) 65–72. http://doi.org/10.1016/j.cep.2019.03.001

[8] S.H. Pyo, M. Sayed, R. Hatti-Kaul, Org. Process Res. Dev. 23 (2019) 952–960. http://doi.org/10.1021/acs.oprd.9b00044

[9] Q.S. Kong, X.-L. Li, H._J. Xu, Y. Fu, Fuel Process. Technol. 209 (2020) 106528–106548. https://doi.org/10.1016/j.fuproc.2020.106528

[10] H. Liu, X. Cao, T. Wang, J. Wei, X. Tang, X. Zeng, Y. Sun, T. Lei, S. Liu, L. Lin, J. Ind. Eng. Chem. 77 (2019) 209–214. https://doi.org/10.1016/j.jiec.2019.04.038

[11] F. Liguori, P. Barbaro, N. Calisi, ChemSusChem 12 (2019) 1–7. http://doi.org/10.1002/cssc.201900833

[12] N. Ma, Y. Song, F. Han, G.I.N. Waterhouse, Y. Li, S. Ai, Catal. Sci. Technol. 10 (2020) 4010–4018. http://doi.org/10.1039/D0CY00363H

[13] X. Wang, X. Liang, J. Li, Q. Li, Appl. Catal. A: Gen. 576 (2019) 85–95. http://doi.org/10.1016/j.apcata.2019.03.005

[14] S. Fulignati, C. Antonetti, D. Licursi, M. Pieraccioni, E. Wilbers, H.J. Heeres, A.M. Raspolli Galletti, Appl. Catal. A: Gen. 578 (2019) 122–133. http://doi.org/10.1016/j.apcata.2019.04.007

[15] T. Wang, J. Wei, H. Liu, Y. Feng, X. Tang, X. Zeng, Y. Sun, T. Lei, L. Lin, J. Ind. Eng. Chem. 81 (2020) 93–98. https://doi.org/10.1016/j.jiec.2019.08.057

[16] D. Maniar, Y. Jiang, A.J.J. Woortman, J. Van Dijken, K. Loos, ChemSusChem 12 (2019) 990–999. https://doi.org/10.1002/cssc.201802867

[17] T. Buntara, S. Noel, P.H. Phua, I. Melián-Cabrera, J.G. De Vries, H.J. Heeres, Angew. Chem. Int. Ed. 50 (2011) 7083–7087. http://doi.org/10.1002/anie.201102156

[18] J. He, S.P. Burt, M. Ball, D. Zhao, I. Hermans, J.A. Dumesic, G.W. Hubert, ACS Catal. 8 (2018) 1427–1439. http://doi.org/10.1021/acscatal.7b03593

[19] B. Xiao, M. Zheng, X. Li, J. Pang, R. Sun, H. Wang, X. Pang, A. Wang, X. Wang, T. Zhang, Green Chem. 18 (2016) 2175–2184. http://doi.org/10.1039/C5GC02228B

[20] D.K. Mishra, H.J. Lee, C.C. Truong, J. Kim, J. Suh, Y.W. Baek, Y.J. Kim, Mol. Catal. 484 (2020) 110722–110730. https://doi:10.1016/j.mcat.2019.110722

[21] K.T.V. Rao, Y. Hu, Z. Yuan, Y. Zhang, C.C. Xu, Appl. Catal. A Gen. 609 (2021) 117892–117903. https://doi.org/10.1016/j.apcata.2020.117892

[22] E. Soszka, M. Jędrzejczyk, I. Kocemba, N. Keller, A.M. Ruppert, Catalysts 10 (2020) 1026–1043. https://doi.org/10.3390/catal10091026

[23] S.G. Newman, K.F. Jensen, Green Chem. 15 (2013) 1465–1472. http://doi.org/10.1039/C3GC40374B

[24] F.M. Akwi, P. Watts, Chem. Commun. 54 (2018) 13894–13928. http://doi.org/10.1039/C8CC07427E

[25] N. Kockmann, P. Thenée, C. Fleischer-Trebes, G. Laudadio, T. Noël, React. Chem. Eng. 2 (2017) 258–280. http://doi.org/10.1039/C7RE00021A

[26] M. Irfan, T.N. Glasnov, C.O. Kappe, ChemSusChem 4 (2011) 300–316. http://doi.org/10.1002/cssc.201000354

[27] A. Hommes, H.J. Heeres, J. Yue, ChemCatChem 11 (2019) 4671–4708. http://doi.org/10.1002/cctc.201900807

[28] M. Kondeboina, S.S. Enumula, K.S. Reddy, P. Challa, D.R. Burri, S.R.R. Kamaraju, Fuel 285 (2021) 119094–119102. https://doi.org/10.1016/j.fuel.2020.119094

[29] A.S. Piskun, J.E. De Haan, E. Wilbers, H.H. Van de Bonekamp, Z. Tang, H.J. Heeres, ACS Sustainable Chem. Eng. 4 (2016) 2939—2950. http://doi.org/10.1021/acssuschemeng.5b00774

[30] B. Mallesham, P. Sudarsanam, B.V.S. Reddy, B.G. Rao, B.M. Reddy, ACS Omega 3 (2018) 1639–16849. https://doi.org/10.1021/acsomega.8b02008

[31] H.R. Prakruthi, B.M. Chandrashekara, B.S. Jai Prakash, Y.S. Bhat, J. Ind. Eng. Chem. 62 (2018) 96–105. https://doi.org/10.1016/j.jiec.2017.12.048

[32] M. Pirmoradi, N. Janulaitis, R.J. Gulotty, J.R. Kastner, Ind. Eng. Chem. Res. 59 (2020) 17748–17761. https://dx.doi.org/10.1021/acs.iecr.0c02866

[33] R. Huang, Q. Cui, Q. Yuan, H. Wu, Y. Guan, P. Wu, ACS Sustainable Chem. Eng. 6 (2018) 6957–6964. http://doi.org/10.1021/acssuschemeng.8b00801

[34] C.M. Mani, M. Braun, V. Molinari, M. Antonietti, N. Fechler, ChemCatChem 9 (2017) 3388–3394. http://doi.org/10.1002/cctc.201700506

[35] G.Y. Jeong, A.K. Singh, S. Sharma, K.W. Gyak, R.A. Maurya, D.P. Kim, NPG Asia Materials 7 (2015) e173. http://doi.org/10.1038/am.2015.21

[36] D.P. Duarte, R. Martínez, L.J. Hoyos, Ind. Eng. Chem. Res. 55 (2016) 54–63. http://doi.org/10.1021/acs.iecr.5b02851

[37] J. Luo, L. Arroyo-Ramírez, J. Wei, H. Yun, C.B. Murray, R.J. Gorte, Appl. Catal. A: Gen. 508 (2015) 86–93. http://doi.org/10.1016/j.apcata.2015.10.009

[38] N. Viar, J.M. Requies, I. Agirre, A. Iriondo, P.L. Arias, Energy 172 (2019) 531–544. https://doi.org/10.1016/j.energy.2019.01.109

[39] A.J. Kumalaputri, G. Bottari, P.M. Erne, H.J. Heeres, K. Barta, ChemSusChem 7 (2014) 2266–2275. https://doi.org/10.1002/cssc.201402095

[40] D. Hu, H. Hu, H. Zhou, G. Li, C. Chen, J. Zhang, Y. Yang, Y. Hu, Y. Zhang, L. Wang, Catal. Sci. Technol. 8 (2018) 6091–6099. http://doi.org/10.1039/C8CY02017E

[41] S. Lima, D. Chadwick, K. Hellgardt, RSC Adv. 7 (2017) 31401–31407. http://doi.org/10.1039/C7RA03318D

[42] J. Luo, L. Arroyo-Ramìrez, R.J. Gorte, D. Tzoulaki, D.G. Vlachos, AIChE Journal 61 (2015) 590–597. https://doi.org/10.1002/aic.14660

[43] D. Licursi, C. Antonetti, S. Fulignati, M. Giannoni, A.M. Raspolli Galletti, Catalysts 8 (2018) 277–292. https://doi.org/10.3390/catal8070277

[44] S. Rivas, A.M. Raspolli Galletti, C.Antonetti, D. Licursi, V. Santos, J.C. Parajó, Catalysts 8 (2018) 169–184. http://doi.org/10.3390/catal8040169

[45] Q. Meng, D. Cao, G. Zhao, C. Qiu, X. Liu, X. Wen, Y. Zhu, Y. Li, Appl. Catal B: Environ. 212 (2017) 15–22. http://doi.org/10.1016/apcatb.2017.04.069

[46] K. Tomishige, Y. Nakagawa, M. Tamura, Green Chem. 19 (2017) 2876–2924. http://doi.org/10.1039/C7GC00620A

[47] D. Götz, M. Lucas, P. Claus, React. Chem. Eng. 1 (2016) 161–164. http://doi.org/10.1039/C5RE00026B

[48] Y. Yang, Z. Du, J. Ma, F. Lu, J. Zhang, J. Xu, ChemSusChem 7 (2014) 1352–1356. http://dx.doi.org/10.1002/cssc.201301270

[49] R.R. Gonzales, Y. Hong, J.H. Park, G. Kumar, S.H. Kim, J. Chem. Technol. Biotechnol. 91 (2016) 1157-1163. http://doi.org/10.1002/jctb.4701

[50] N. Al-Raifi, F. Galvanin, M. Morad, E. Cao, S. Cattaneo, M. Sankar, V. Dua, G. Hutchings, A. Gavriilidis, Chem. Eng. Sci. 149 (2016) 129-142. http://doi.org/10.1016/j.ces.2016.03.018

[51] B. Girisuta, L.P.B.M. Janssen, H.J. Heeres, Green Chem. 8 (2006) 701-709. http://doi.org/10.1039/B518176C

[52] B. Kuang, Q. Zhang, Y. Fang, Y. Bai, S. Qiu, P. Wu, Y. Qin, T. Wang, Ind. Eng. Chem. Res. 59 (2020) 9372–9381. http://doi.org/10.1039/C7GC00620A

[53] T.P. Sulmonetti, B. Hu, S. Lee, P.K. Agrawal, C.W. Jones, ACS Sustainable Chem. Eng. 5 (2017) 8959–8969. http://doi.org/10.1021/acssuschemeng.7b01769

[54] T. Buntara, I. Melián-Cabrera, Q. Tan, J.L.G. Fierro, M. Neurock, J.G. de Vries, H.J. Heeres, Catal. Today 210 (2013) 106–116. http://doi.org/10.1016/j.cattod.2013.04.012

[55] J. He, S.P. Burt, M.R. Ball, I. Hermans, J.A. Dumesic, G.W. Huber, Appl. Catal. B. Env. 258 (2019) 117945–117954. https://doi.org/10.1016/j.apcatb.2019.117945

[56] S. Liu, Bioprocess Engineering: kinetics, sustainability, and reactor design, Elsevier, Amsterdam, 2017.

[57] M.A. Vannice, Kinetics of catalytic reactions, Springer, New York, 2005.

[58] C. Moreno-Marrodan, P. Barbaro, Green Chem. 16 (2014) 3434–3438. http://doi.org/10.1039/C4GC00298A

[59] S. Iqbal, S.A. Kondrat, D.R. Jones, D.C. Schoenmakers, J.K. Edwards, L. Lu, B.R. Yeo, P.P. Wells, E.K. Gibson, D.J. Morgan, C.J. Kiely, G.J. Hutchings, ACS Catal. 5 (2015) 5047–5059. http://doi.org/10.1021/acscatal.5b00625

[60] O.A. Abdelrahman, A. Heyden, J.Q. Bond, ACS Catal. 4 (2014) 1171–1181. http://doi.org/10.1021/cs401177p

[61] E.P. Maris, W.C. Ketchie, V. Oleshko, R.J. Davis, J. Phys. Chem. B 110 (2006) 7869–7876. http://doi.org/10.1021/jp057022y

Caption for figures and schemes

Figure 1 Concentrations versus time-on-stream for the continuous HMF hydrogenation up to 50 h (A) and up to 6 h (B). Reaction conditions: T = 100 °C; P = 50 bar; [HMF] = 0.1 wt%; H_2 flow = 100 ml/min; liquid flow = 1 ml/min; catalyst contact time = 10 g_{cat}×min/g_{HMF}. Note: where the error bars are not visible, they are smaller than the symbols.

Figure 2 Conversion (X), products yields (Y) and carbon balance versus catalyst contact time. Reaction conditions: T = 100 °C; P = 50 bar; [HMF] = 7.9 mM; H_2 flow = 100 ml/min; liquid flow = 1 ml/min.

Figure 3 Conversion (X), products yields (Y) and carbon balance versus temperature at catalyst contact time of 20 g_{cat}×min/g_{HMF} (A) and 300 g_{cat}×min/g_{HMF} (B). Reaction conditions: P = 50 bar; [HMF] = 0.1 wt%; H_2 flow = 100 ml/min; liquid flow = 1 ml/min.

Figure 4 Conversion (X), products yields (Y) and carbon balance versus pressure at a catalyst contact time of 20 g_{cat}×min/g_{HMF} (A) and 300 g_{cat}×min/g_{HMF} (B). Reaction conditions: T = 100 °C; [HMF] = 0.1 wt%; H_2 flow = 100 ml/min; liquid flow = 1 ml/min.

Figure 5 Conversion (X), products yields (Y) and carbon balance versus HMF feed concentration with a catalyst intake of 0.02 g (A) and 0.30 g (B). Reaction conditions: T = 100 °C; P = 50 bar; H_2 flow = 100 ml/min; liquid flow = 1 ml/min.

Figure 6 Conversion (X) in the presence of different catalyst particle sizes: 25-75 μm (A) and 150-200 μm (B). Reaction conditions: catalyst contact time = 10 g_{cat}×min/g_{HMF}; T = 100 °C; P = 50 bar; H_2 flow = 100 ml/min; liquid flow = 1 ml/min.

Figure 7 HMF conversion (X), products yields (Y) and carbon balance in the presence of the fresh catalyst and after two recycles. Reaction conditions: catalyst contact time = 10 g_{cat}×min/g_{HMF} T = 100 °C; P = 50 bar; [HMF] = 0.1 wt%; H_2 flow = 100 ml/min; liquid flow = 1 ml/min.

Scheme 1 Conversion of HMF to the desired products BHMF and BHMTHF.

Table 1: Overview of the literature on the HMF hydrogenation carried out in flow reactors.

Catalyst	Solvent	Reaction conditions	Catalyst contact time (g_{cat}×min/g_{HMF})	C_{HMF} (wt%)	HMF Conversion (mol%)	Product Yield (mol%)	Ref
15 wt% Ni/porous carbon	EtOH	150 °C 6 bar 30 ml/min H_2	50	0.6	79	68[a]	34
Ru/Cu/Fe_3O_4/ N-rGO[b]	DMSO	150 °C 8 bar 47 ml/min H_2	1000	5.4	100	91[a]	35
0.7 wt% Pd/Al_2O_3	H_2O	189 °C 4 bar 50 ml/min H_2	400	5.0	100	13[a]	36
10 wt% Pt/C	1-PrOH	180 °C 33 bar 20 ml/min H_2	25	1.2	85	50[a]	37
7.6 wt% Cu-PMO	EtOH	100 °C 50 bar 30 ml/min H_2	54	0.5	90	80[c]	38
5 wt% Cu/Al_2O_3 doped with 1.5 wt% K	EtOH	120 °C 20 bar 50 ml/min H_2	60	3.0	100	99[c]	39
RANEY Cu	H_2O	90 °C 90 bar n.a.[d]	280	1.0	n.a.[d]	86[c]	40
1) RANEY Cu 2) RANEY Ni	H_2O	90 °C 90 bar n.a.[d]	280	1.0	n.a.[d]	76[e]	40
0.6 wt% Pd/SiO_2	H_2O	100 °C 30 bar 60 ml/min H_2	1000	1.0	100	100[e]	19

[a] DMF
[b] Bimetallic Ru and Cu loaded on N-doped reduced graphene oxide with iron oxide
[c] BHMF
[d] n.a. = not available
[e] BHMTHF

Table 2: Process parameters and their values/ranges.

Process parameters	Units	Ranges
Liquid flow	ml/min	1
Catalyst contact time	$g_{cat} \times min/g_{HMF}$	10–300
Temperature	°C	60–120
Hydrogen pressure	bar	10–50
Hydrogen flow	ml/min	30–130
HMF inlet concentration	wt%	0.1–2.0
	mM	7.9–158.0
Time-on-stream	h	1–50

Supplementary Data

Tunable HMF hydrogenation to furan diols in a flow reactor using Ru/C as catalyst

Sara Fulignati[a], Claudia Antonetti[a]*, Erwin Wilbers[b], Domenico Licursi[a], Hero Jan Heeres[b], Anna Maria Raspolli Galletti[a]

[a] *Department of Chemistry and Industrial Chemistry, University of Pisa, Via G. Moruzzi 13, 56124, Pisa, Italy.*

[b] *Green Chemical Reaction Engineering, ENTEG, University of Groningen, Nijenborgh 4, 9747 AG Groningen, The Netherlands.*

*Corresponding author, e-mail: claudia.antonetti@unipi.it

Set-up of flow reactor

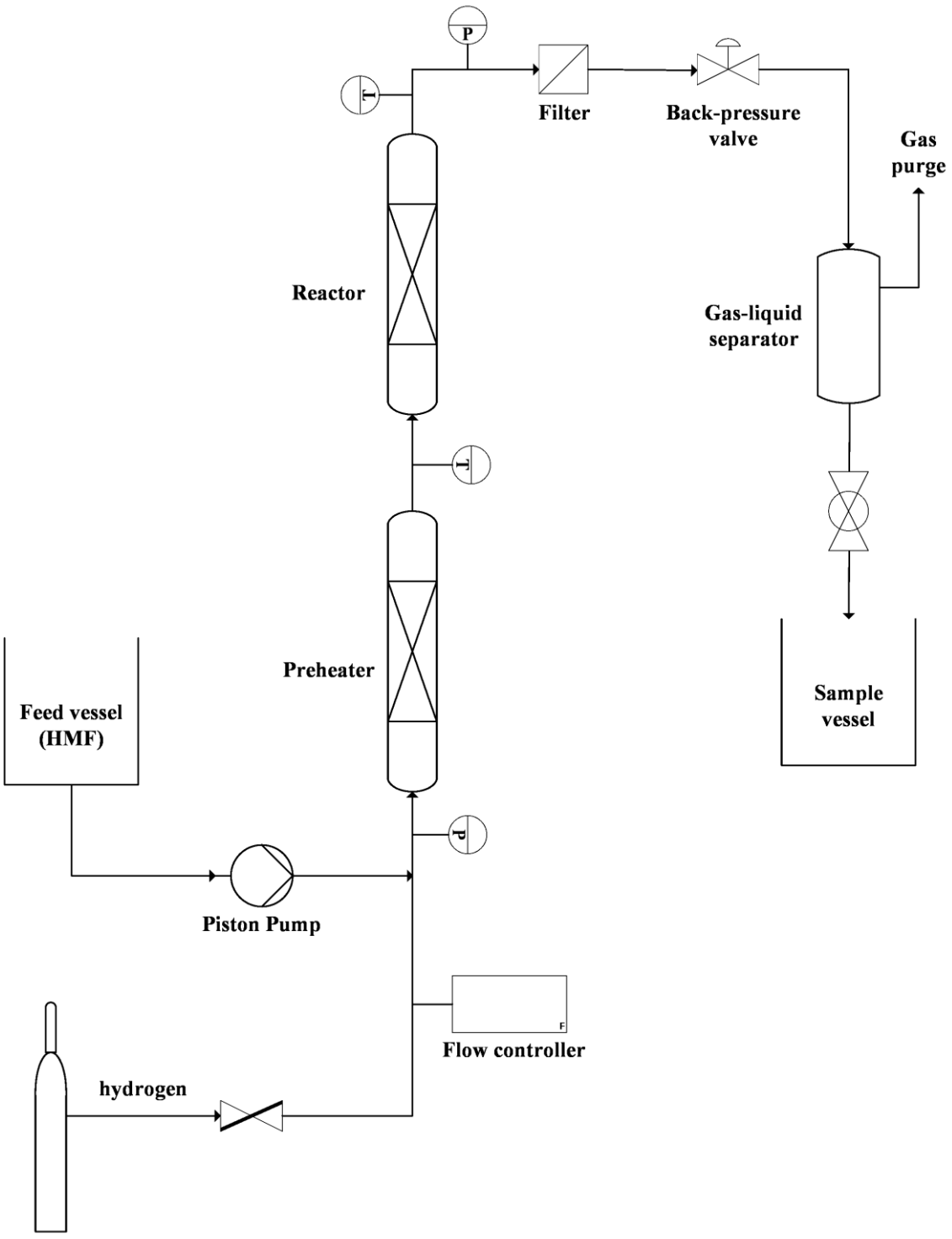

Scheme S1: Set-up of flow reactor.

Scheme of formation of tetrahydrofurfuryl alcohol and 1,2-pentandiol from HMF and BHMTHF

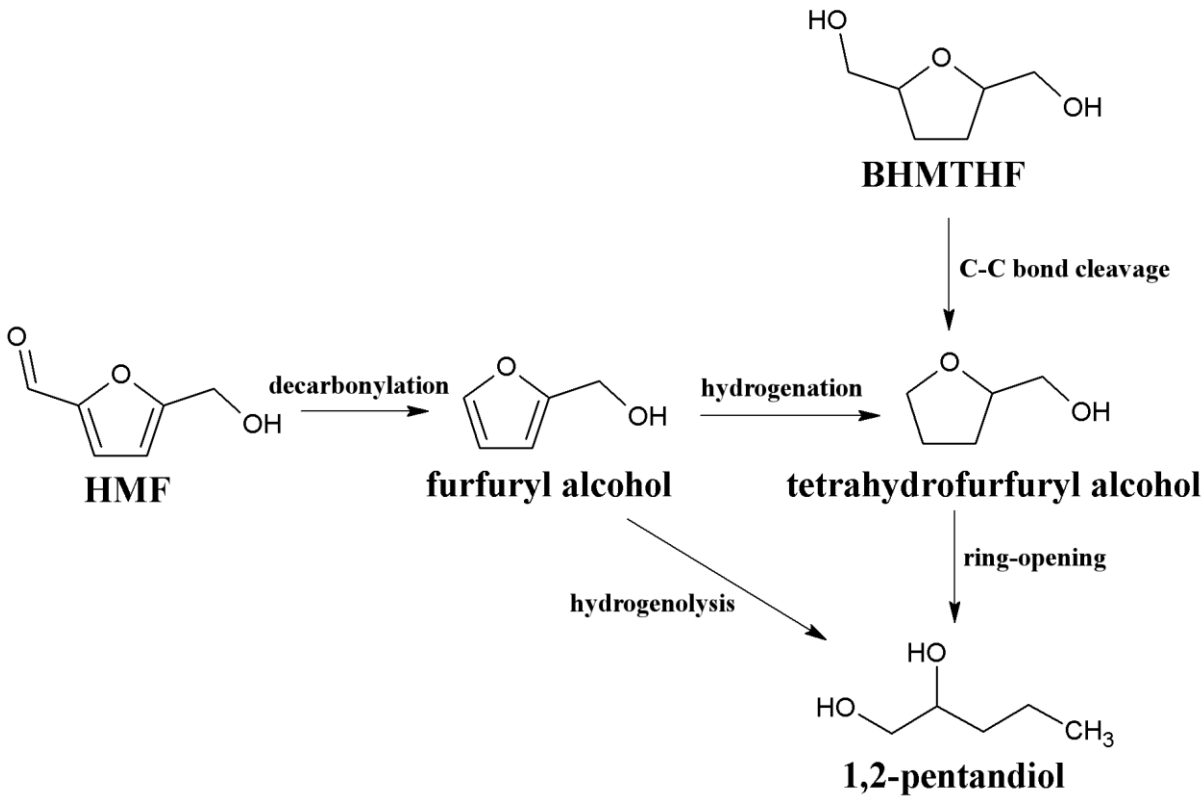

Scheme S2: Formation of tetrahydrofurfuryl alcohol and 1,2-pentandiol from HMF and BHMTHF.

Profile of conversion, products yields and carbon balance versus H_2 flow rate at different catalyst contact time

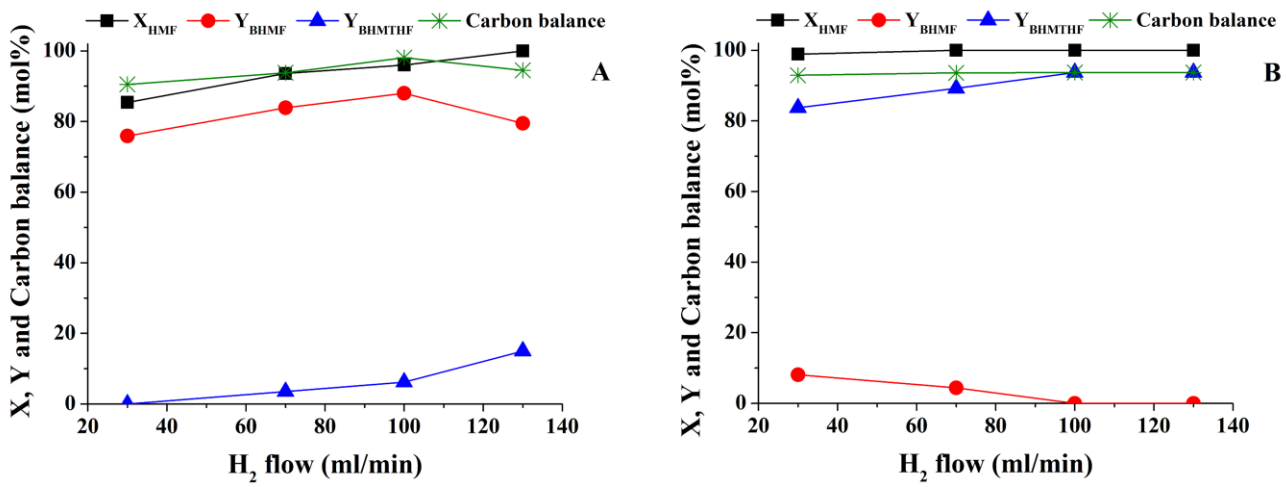

Figure S1: Profile of conversion (X), products yields (Y) and carbon balance versus H_2 flow rate at catalyst contact time of 20 g_{cat}×min/g_{HMF} (A) and 300 g_{cat}×min/g_{HMF} (B). Reaction conditions: T = 100 °C; P = 50 bar; [HMF] = 0.1 wt%; liquid flow = 1 ml/min.

Possible pathways of the HMF and BHMTHF decomposition at high HMF concentration

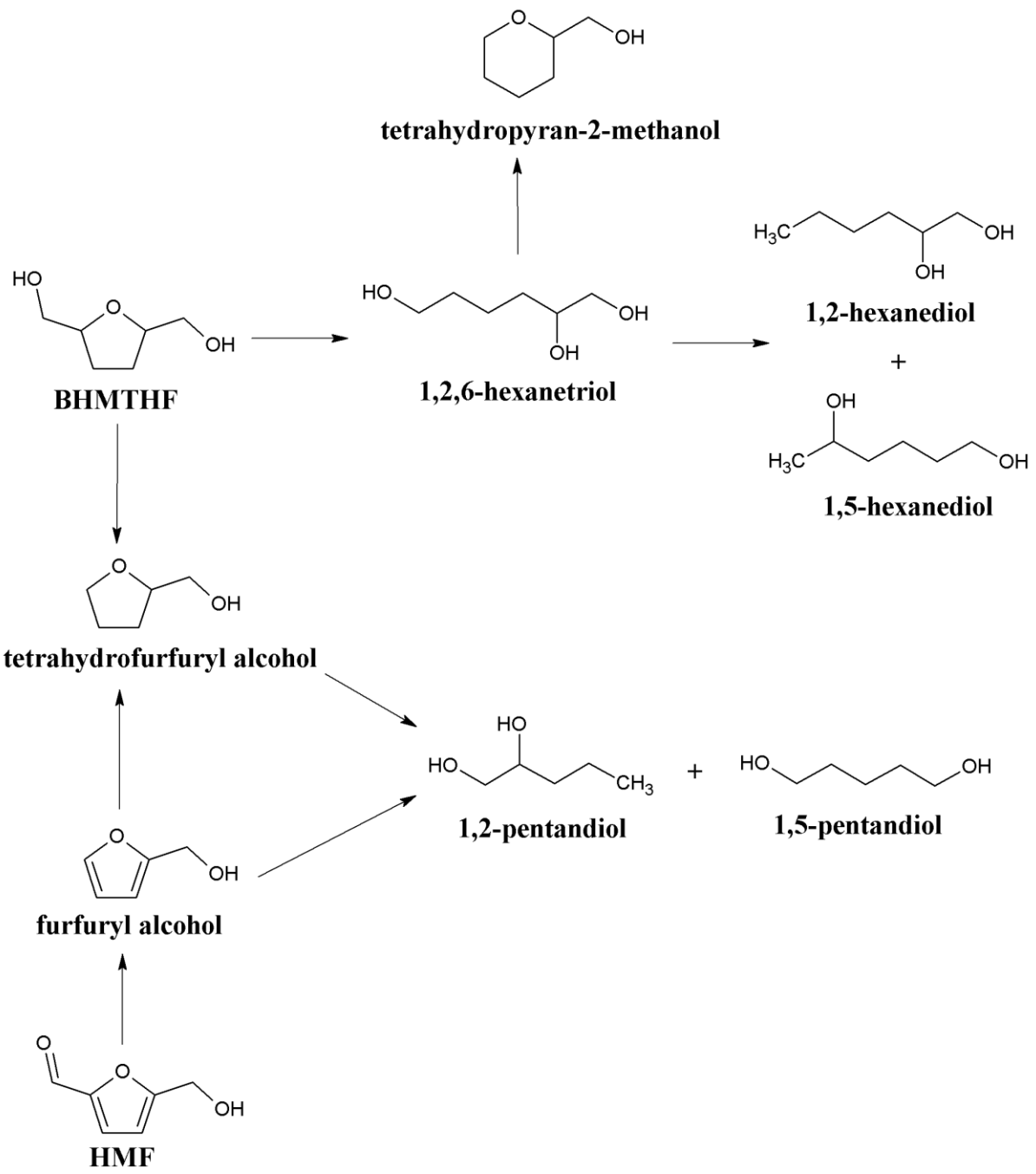

Scheme S3: Possible pathways for HMF and BHMTHF decomposition at high HMF concentration. Reaction conditions: T = 100 °C; P = 50 bar; H_2 flow = 100 ml/min; liquid flow = 1 ml/min; reactor space time = 300 g_{cat}×min/g_{HMF}.

Calculations of intraparticle diffusion of HMF and hydrogen

Assessment of the N_{WP} criterion for HMF

1) radius of the catalyst particle (r_p): according to the supplier information, the particle size distribution is the following one:

d_{10} = 5 μm (10% of all particles are smaller than 5 μm)

d_{50}= 25 μm (50% of all particles are smaller than 25 μm)

d_{90} = 75 μm (90% of all particles are smaller than 75 μm)

We can suppose the mean value for the particle diameter between 75 and 25 μm, thus an average radius of 2.5×10^{-5} m was considered.

2) concentration of HMF at the catalyst surface (C_s): we supposed that the concentration of HMF on the particle surface was an average between the starting concentration (0.1 wt%, which corresponds to 7.9 mol/m^3) and that reached at the steady state, determined on the basis of the HMF conversion.

3) effective diffusion coefficient (D_{eff}): the diffusion coefficient of HMF in water was estimated trough the Wilke-Chang equation (eq. S1) [1,2]:

$$D_{AB} = [7.4 \times 10^{-8} \times T \times (\phi_B \times M_B)^{0.5}]/(V_{bA}^{0.6} \times \mu) \qquad \text{(eq. S1)}$$

Where the symbols with subscript A are referred to the solute (HMF), with B to the solvent (H_2O):

- D_{AB} is the diffusivity of HMF in very dilute H_2O solution, cm^2/s;
- M_B is the molecular weight of H_2O, g/mol;
- T is the temperature, K;
- μ is the viscosity of H_2O, cP;
- V_{bA} is the HMF molar volume at its normal boiling point, cm^3/mol. It was calculated according to the generalized correlation proposed by Maloka regarding the liquid

molar volume at the normal boiling point [3] and the calculated value was equal to 119.7 cm^3/mol;

- ϕ_B is the association factor of H_2O (2.6) [1].

The effective diffusion coefficient (D_{eff}) was considered as 10% of the diffusion coefficient, according to the Wilke-Chang equation [1,2].

4) experimental reaction rate (R_{exp}): it was determined by the ratio between the molar flow rates of converted HMF (determined at the steady state) and the volume of the employed catalyst, estimated by using the amount of catalyst and its bulk density, provided by the supplier and equal to 750 kg/m^3.

Assessment of the N_{WP} criterion for hydrogen

1) radius of the catalyst particle (r_p): it was the same considered before for HMF.

2) concentration of hydrogen at the catalyst surface (C_s): in this case we considered the bulk concentration of H_2 at the start of the reaction, which results the highest. The H_2 concentration was calculated from the H_2 pressure in the reactor through the Henry law (eq. S2):

$$p = k_H \times C_s \qquad \text{(eq. S2)}$$

where:

- p is the partial pressure of H_2 above the solution (atm);
- C_s is the concentration of the dissolved H_2 (mol/l);
- k_H is the Henry's law constant for the gas phase (l×atm/mol), which depends on temperature according to eq. S3:

$$k_{H,T} = k_{H,298} \times \exp\left[-c \times (1/T - 1/298)\right] \qquad \text{(eq. S3)}$$

where:

- $k_{H,298}$ is 1282.05 l×atm/mol [4];

- c is a constant and for H_2 it is 500 K [4].

3) effective diffusion coefficient (D_{eff}): the diffusion coefficient of hydrogen in water was taken from Verhallen et al. [5] and, similarly to HMF, the effective diffusion coefficient was considered as 10% of the diffusion coefficient.

4) experimental reaction rate (R_{exp}): it was the same considered before for HMF.

On these bases, the values of individual contributions of the Weisz-Prater equation and the Weisz-Prater numbers for HMF and hydrogen are reported in Tables S1 and S2, respectively. The values higher than 0.3, representing the reaction where the intraparticle mass transfer limitation is not negligible are evidenced in bold.

Table S1: Calculation of Weisz-Prater number of HMF. Radius of catalyst particles $r_p = 2.5 \times 10^{-5}$ m in all runs.

Run[a]	HMF C_0 (mol/m^3) [wt%]	T (K)	P (bar)	m_{cat} (g)	H_2 flow (ml/min)	X_{HMF} (mol%)	HMF C_s (mol/m^3)	D_{eff} (m^2/s)	R_{exp} (mol/m$^3_{cat}$ × s)	N_{WP} HMF
1	7.9 [0.1]	373	50	0.01	100	62.8	5.4	3.81×10^{-10}	6.4	**1.94**
2	7.9 [0.1]	373	50	0.02	100	96.0	4.1	3.81×10^{-10}	4.8	**1.92**
3	7.9 [0.1]	373	50	0.05	100	100	3.9	3.81×10^{-10}	2.0	**0.84**
4	7.9 [0.1]	373	50	0.15	100	100	3.9	3.81×10^{-10}	0.7	0.29
5	7.9 [0.1]	373	50	0.30	100	100	3.9	3.81×10^{-10}	0.3	0.13
6	7.9 [0.1]	333	50	0.02	100	46.1	6.1	2.06×10^{-10}	2.3	**1.14**
7	7.9 [0.1]	353	50	0.02	100	69.6	5.2	2.86×10^{-10}	3.5	**1.47**
8	7.9 [0.1]	393	50	0.02	100	86.4	4.5	4.88×10^{-10}	4.3	**1.22**
9	7.9 [0.1]	333	50	0.30	100	100	3.9	2.06×10^{-10}	0.3	0.23
10	7.9 [0.1]	353	50	0.30	100	100	3.9	2.86×10^{-10}	0.3	0.17

11	7.9 [0.1]	393	50	0.30	100	100	3.9	4.88×10^{-10}	0.3	0.10
12	7.9 [0.1]	373	10	0.02	100	70.7	5.1	3.81×10^{-10}	3.5	**1.13**
13	7.9 [0.1]	373	30	0.02	100	90.1	4.3	3.81×10^{-10}	4.5	**1.72**
14	7.9 [0.1]	373	40	0.02	100	93.7	4.2	3.81×10^{-10}	4.7	**1.84**
15	7.9 [0.1]	373	10	0.30	100	100	3.9	3.81×10^{-10}	0.3	0.13
16	7.9 [0.1]	373	30	0.30	100	100	3.9	3.81×10^{-10}	0.3	0.13
17	7.9 [0.1]	373	40	0.30	100	100	3.9	3.81×10^{-10}	0.3	0.13
18	7.9 [0.1]	373	50	0.02	30	85.4	4.5	3.81×10^{-10}	4.3	**1.57**
19	7.9 [0.1]	373	50	0.02	70	93.6	4.2	3.81×10^{-10}	4.7	**1.84**
20	7.9 [0.1]	373	50	0.02	130	100	3.9	3.81×10^{-10}	5.0	**2.10**
21	7.9 [0.1]	373	50	0.30	30	98.9	4.0	3.81×10^{-10}	0.3	0.12
22	7.9 [0.1]	373	50	0.30	70	100	3.9	3.81×10^{-10}	0.3	0.13
23	7.9 [0.1]	373	50	0.30	130	100	3.9	3.81×10^{-10}	0.3	0.13
24	39.5 [0.5]	373	50	0.02	100	71.4	25.4	3.81×10^{-10}	18.2	**1.18**
25	79.0 [1.0]	373	50	0.02	100	63.6	53.9	3.81×10^{-10}	31.4	**0.96**
26	158.0 [2.0]	373	50	0.02	100	48.4	119.7	3.81×10^{-10}	47.7	**0.65**
27	39.5 [0.5]	373	50	0.30	100	100	19.8	3.81×10^{-10}	1.7	0.14
28	79.0 [1.0]	373	50	0.30	100	100	39.5	3.81×10^{-10}	3.3	0.14
29	158.0 [2.0]	373	50	0.30	100	100	79.0	3.81×10^{-10}	6.6	0.14

[a] Runs 1 represented in Figure 1 of the manuscript.
Runs 1-5 represented in Figure 2 of the manuscript.
Runs 2,6-8 and 5,9-11 represented in Figure 3A and 3B of the manuscript, respectively.
Runs 2,12-14 and 5,15-17 represented in Figure 4A and 4B of the manuscript, respectively.
Runs 2,18-20 and 5,21-23 represented in Figure S1A and S1B of the S.I., respectively.
Runs 2,24-26 and 5,27-29 represented in Figure 5A and 5B of the manuscript, respectively.

Table S2: Calculation of Weisz-Prater number of H_2. Radius of catalyst particles $r_p = 2.5 \times 10^{-5}$ m in all runs.

Run[a]	HMF C_0 (mol/m^3) [wt%]	T (K)	P (bar)	m_{cat} (g)	H_2 flow (ml/min)	X_{HMF} (mol%)	H_2 C_s (mol/m^3)	D_{eff} (m^2/s)	R_{exp} (mol/m$^3_{cat}$ × s)	N_{WP} H_2
1	7.9 [0.1]	373	50	0.01	100	62.8	27.5	1.79×10^{-9}	6.4	0.08
2	7.9 [0.1]	373	50	0.02	100	96.0	27.5	1.79×10^{-9}	4.8	0.06
3	7.9 [0.1]	373	50	0.05	100	100	27.5	1.79×10^{-9}	2.0	0.03
4	7.9 [0.1]	373	50	0.15	100	100	27.5	1.79×10^{-9}	0.7	0.01
5	7.9 [0.1]	373	50	0.30	100	100	27.5	1.79×10^{-9}	0.3	0.004
6	7.9 [0.1]	333	50	0.02	100	46.1	32.3	9.68×10^{-10}	2.3	0.05
7	7.9 [0.1]	353	50	0.02	100	69.6	29.6	1.35×10^{-9}	3.5	0.05
8	7.9 [0.1]	393	50	0.02	100	86.4	25.7	2.29×10^{-9}	4.3	0.05
9	7.9 [0.1]	333	50	0.30	100	100	32.3	9.68×10^{-10}	0.3	0.006
10	7.9 [0.1]	353	50	0.30	100	100	29.6	1.35×10^{-9}	0.3	0.005
11	7.9 [0.1]	393	50	0.30	100	100	25.7	2.29×10^{-9}	0.3	0.003
12	7.9 [0.1]	373	10	0.02	100	70.7	5.5	1.79×10^{-9}	3.5	0.22
13	7.9 [0.1]	373	30	0.02	100	90.1	16.5	1.79×10^{-9}	4.5	0.10
14	7.9 [0.1]	373	40	0.02	100	93.7	22.0	1.79×10^{-9}	4.7	0.07
15	7.9 [0.1]	373	10	0.30	100	100	5.5	1.79×10^{-9}	0.3	0.02
16	7.9 [0.1]	373	30	0.30	100	100	16.5	1.79×10^{-9}	0.3	0.006
17	7.9 [0.1]	373	40	0.30	100	100	22.0	1.79×10^{-9}	0.3	0.005
18	7.9 [0.1]	373	50	0.02	30	85.4	27.5	1.79×10^{-9}	4.3	0.05
19	7.9	373	50	0.02	70	93.6	27.5	1.79×10^{-9}	4.7	0.06

	[0.1]									
20	7.9 [0.1]	373	50	0.02	130	100	27.5	1.79×10^{-9}	5.0	0.06
21	7.9 [0.1]	373	50	0.30	30	98.9	27.5	1.79×10^{-9}	0.3	0.004
22	7.9 [0.1]	373	50	0.30	70	100	27.5	1.79×10^{-9}	0.3	0.004
23	7.9 [0.1]	373	50	0.30	130	100	27.5	1.79×10^{-9}	0.3	0.004
24	39.5 [0.5]	373	50	0.02	100	71.4	27.5	1.79×10^{-9}	18.2	0.23
25	79.0 [1.0]	373	50	0.02	100	63.6	27.5	1.79×10^{-9}	31.4	**0.40**
26	158.0 [2.0]	373	50	0.02	100	48.4	27.5	1.79×10^{-9}	47.7	**0.61**
27	39.5 [0.5]	373	50	0.30	100	100	27.5	1.79×10^{-9}	1.7	0.02
28	79.0 [1.0]	373	50	0.30	100	100	27.5	1.79×10^{-9}	3.3	0.04
29	158.0 [2.0]	373	50	0.30	100	100	27.5	1.79×10^{-9}	6.6	0.08

[a] Runs 1 represented in Figure 1 of the manuscript.
Runs 1-5 represented in Figure 2 of the manuscript.
Runs 2,6-8 and 5,9-11 represented in Figure 3A and 3B of the manuscript, respectively.
Runs 2,12-14 and 5,15-17 represented in Figure 4A and 4B of the manuscript, respectively.
Runs 2,18-20 and 5,21-23 represented in Figure S1A and S1B of the S.I., respectively.
Runs 2,24-26 and 5,27-29 represented in Figure 5A and 5B of the manuscript, respectively.

TEM analysis of fresh and spent Ru/C

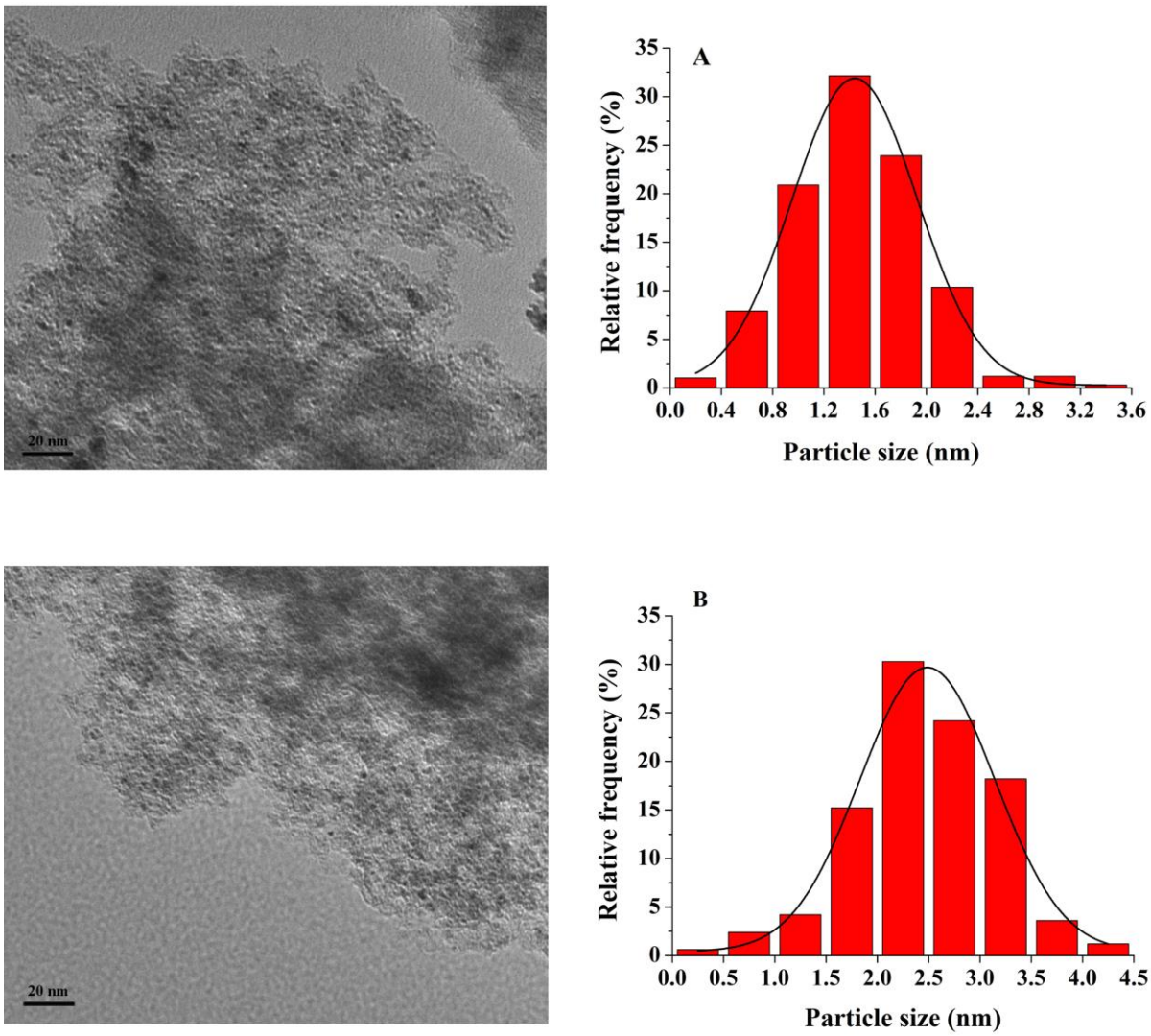

Figure S2: TEM pictures of fresh Ru/C (A) and spent Ru/C (B) employed in the experiment of Figure 1 with the respective distribution of the Ru particle sizes and the Gaussian fitting.

References

[1] C.R. Wilke, P. Chang, AIChe J. 1 (1955) 264–270. https://doi.org/10.1002/aic690010222

[2] R. Sitaraman, S.H. Ibrahim, N.R. Kuloor, J. Chem. Eng. Data 8 (1963) 198–201. https://doi.org/10.1021/je60017a017

[3] I.E. Maloka, Pet. Sci. Technol. 23 (2005) 133–136. https://doi.org/10.1081/LFT-200028058

[4] A.S. Piskun, J.E. de Haan, E. Wilbers, H.H. van de Bovenkamp, Z. Tang, H.J. Heeres, ACS Sustainable Chem. Eng. 4 (2016) 2939–2950. https://doi.org/10.1021/acssuschemeng.5b00774

[5] P.T.H.M. Verhallen, L.J.P. Oomen, A.J.J.M. Elsen, A.J. Kruger, Chem. Eng. Sci. 39 (1984) 1535–1541. https://doi.org/10.1016/0009-2509(84)80082-2

Figure 1

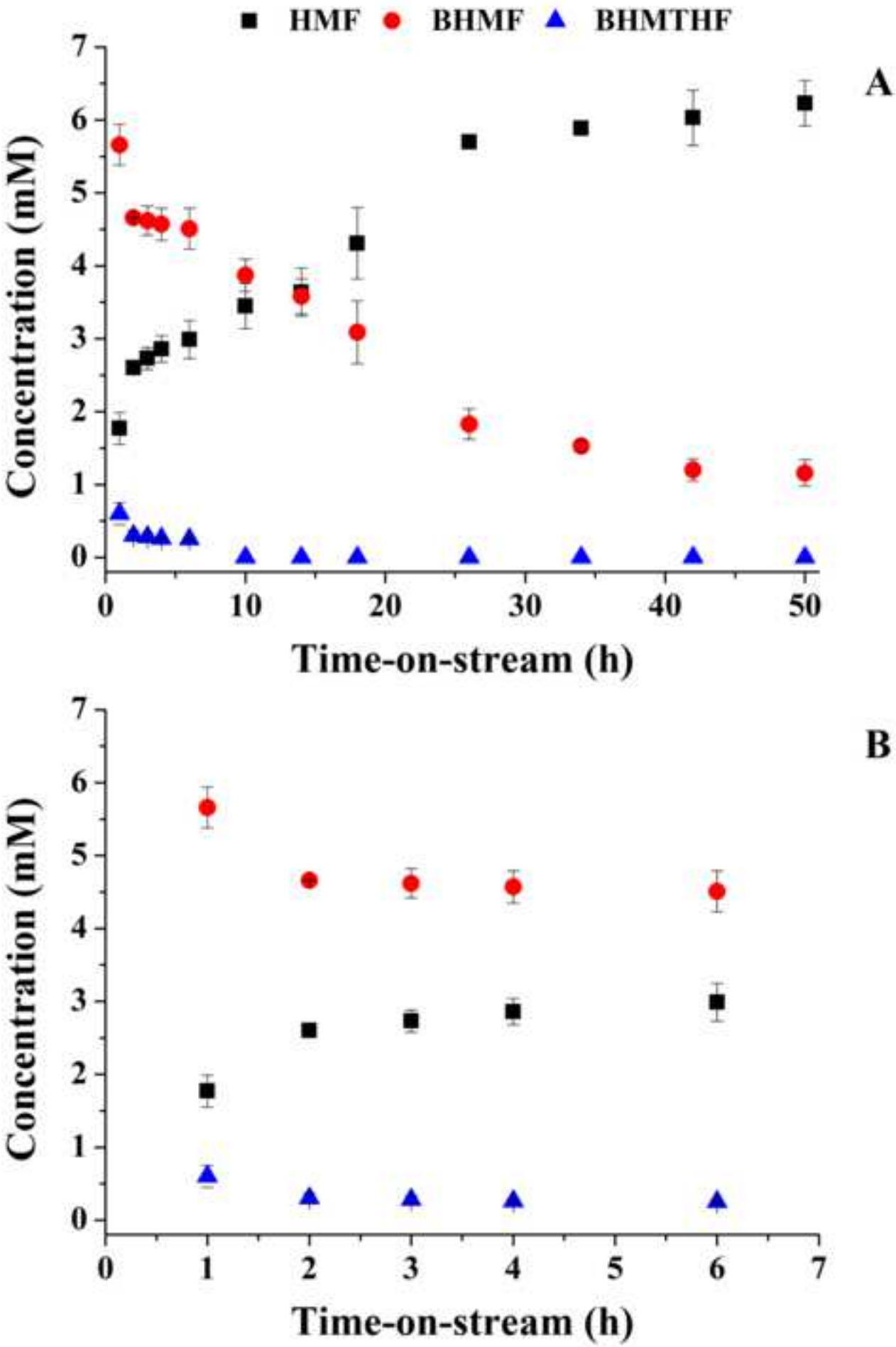

Figure 2

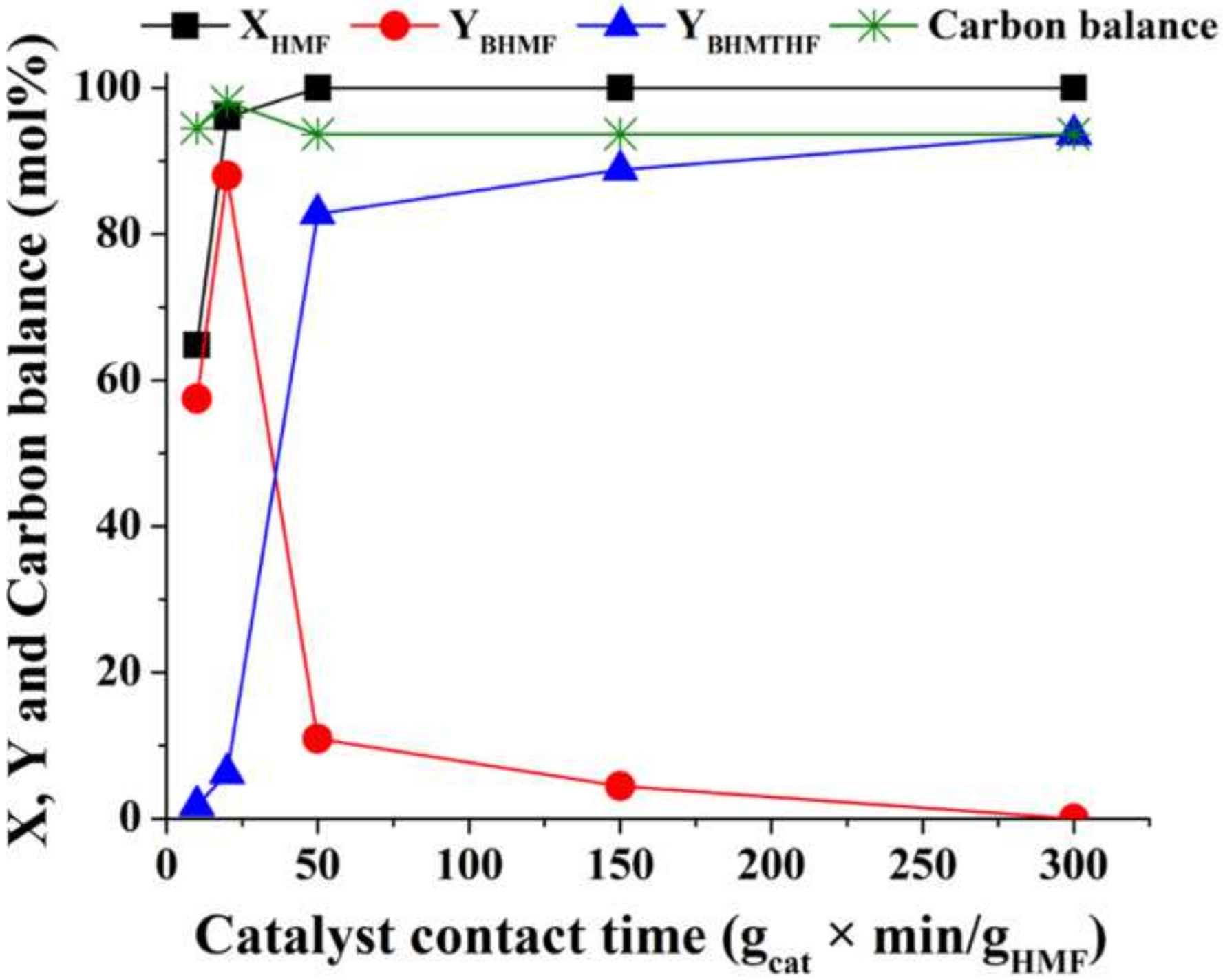

Figure 3

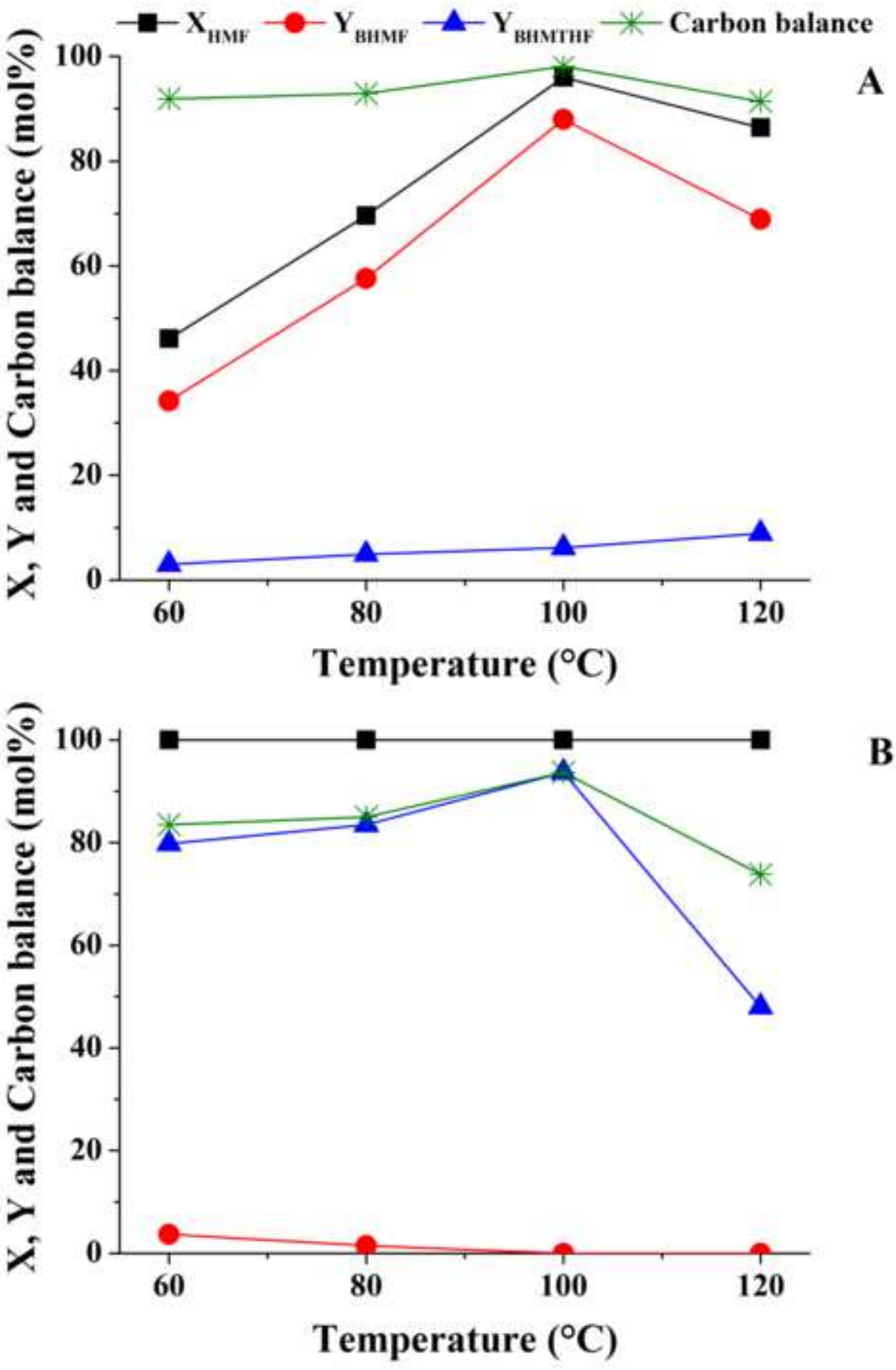

Figure 4

Click here to access/download;Figure;Figure 4.tif

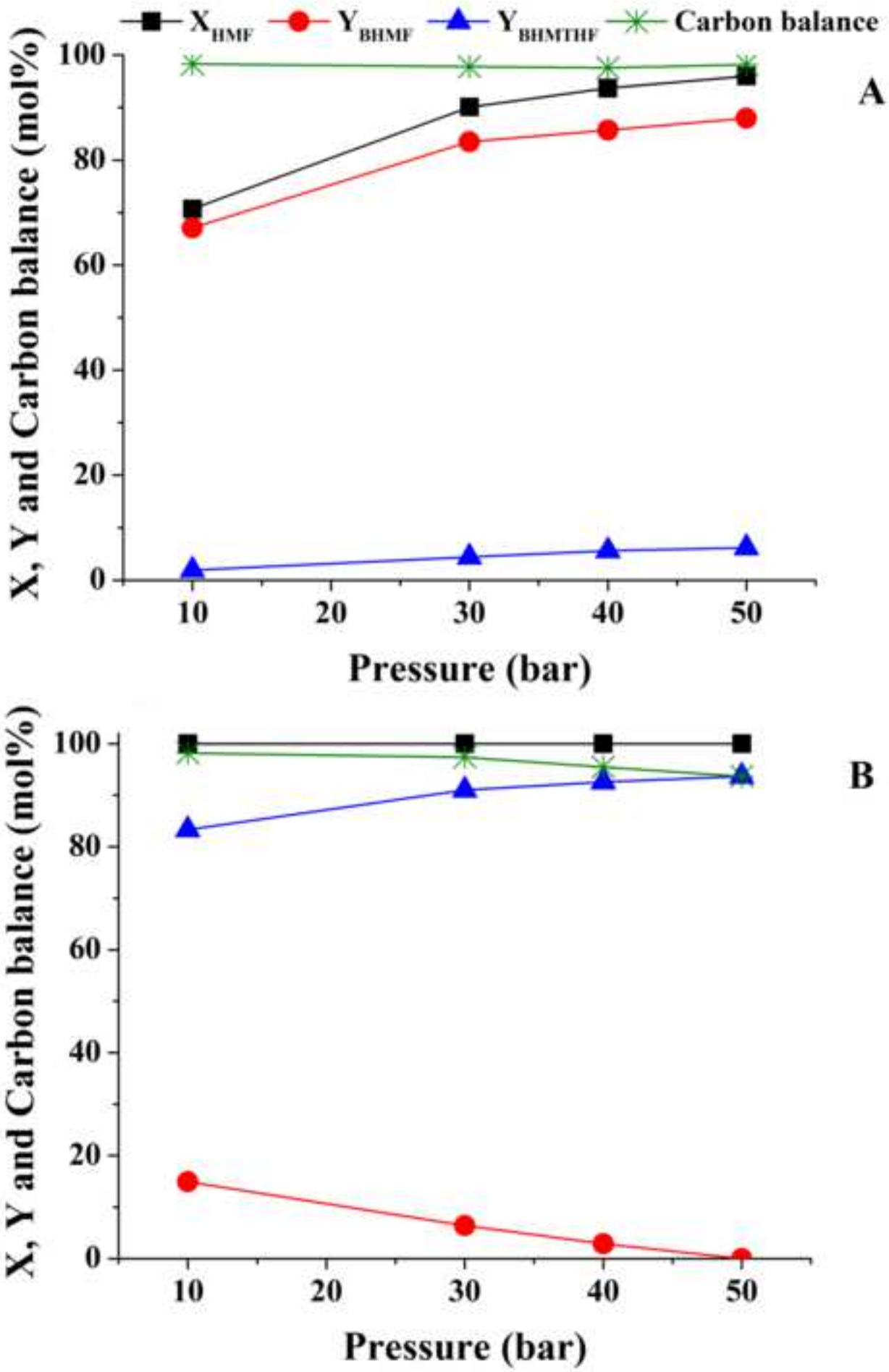

Figure 5

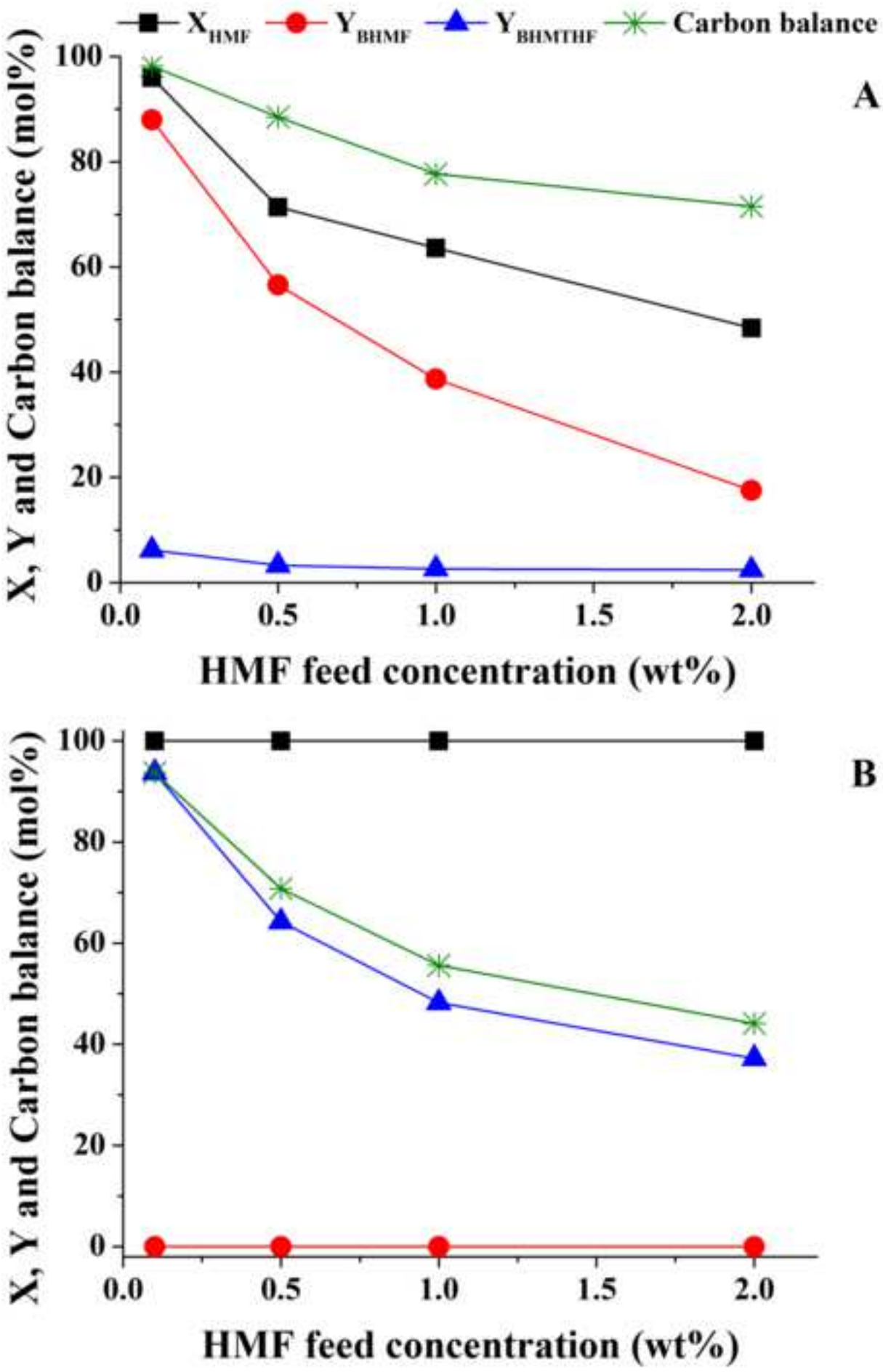

Figure 6

Click here to access/download;Figure;Figure 6.tif

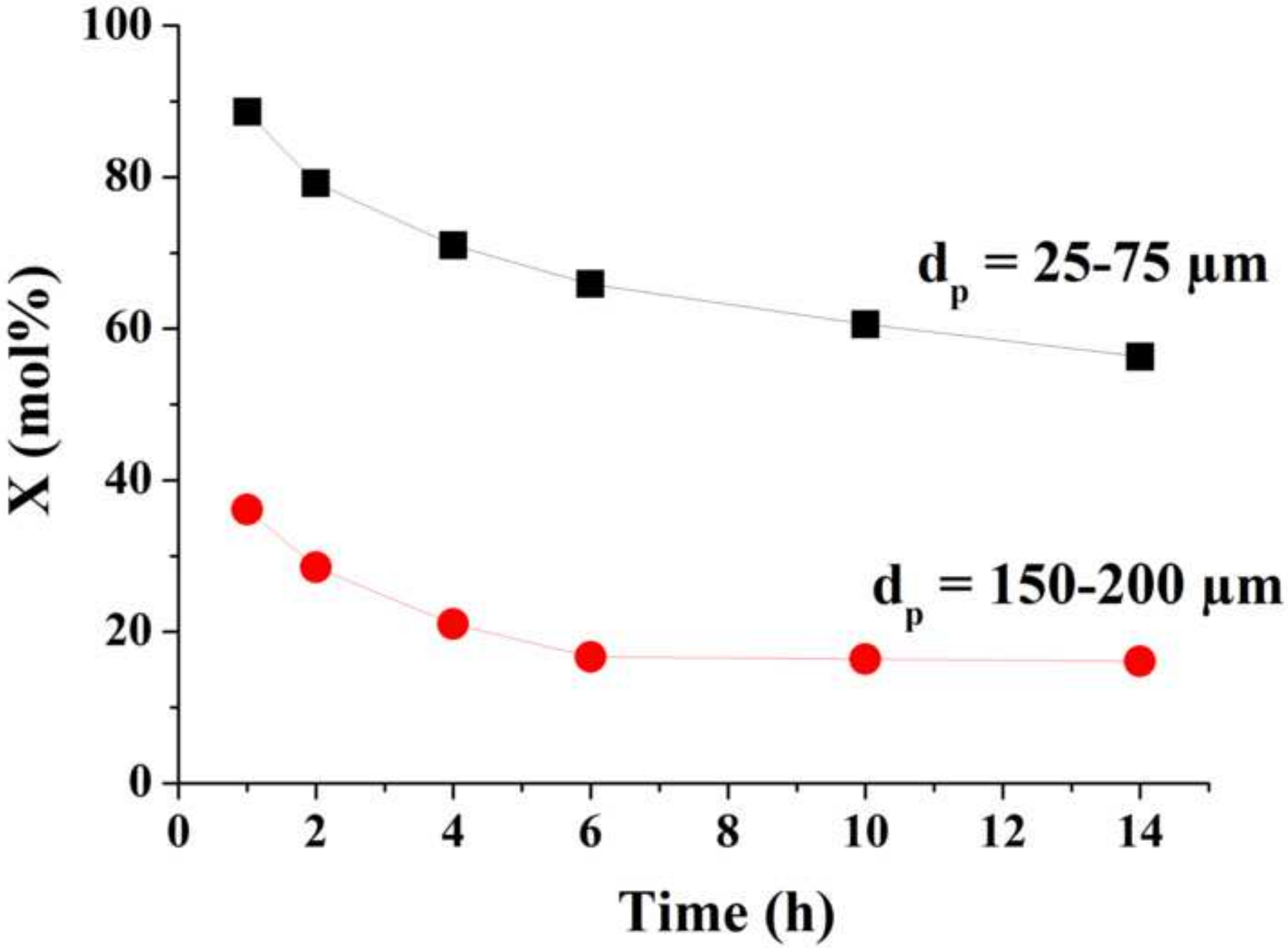

Figure 7

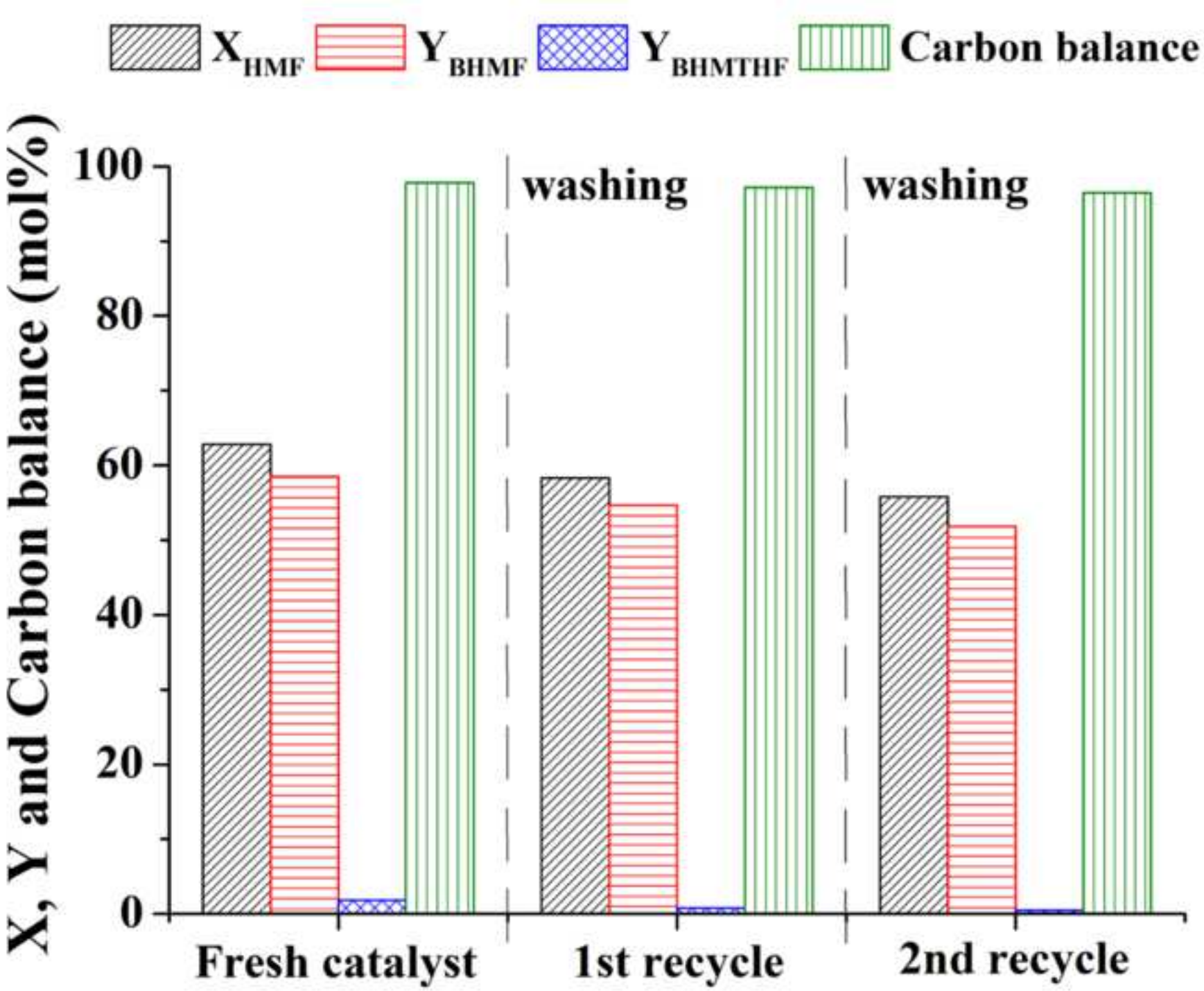

Scheme 1

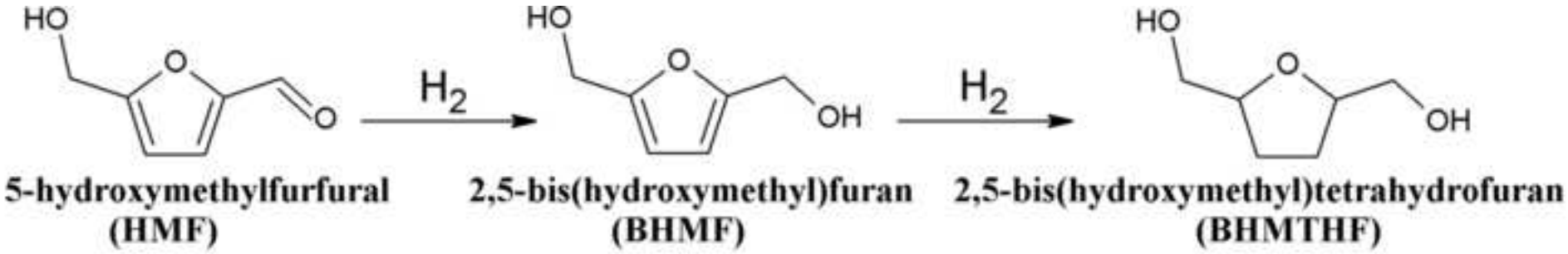

5-hydroxymethylfurfural (HMF) → **2,5-bis(hydroxymethyl)furan (BHMF)** → **2,5-bis(hydroxymethyl)tetrahydrofuran (BHMTHF)**